Earth and Environmental Science Transactions of the Royal Society of Edinburgh, **115**, 113–129, 2024

Spontaneous Article

The early actinopterygian genus *Rhadinichthys* redefined, the type species *ornatissimus* redescribed, and the species *bearsdeni* introduced

Yunyan MO[1], Abigail M. CARON[2] and Michael I. COATES[3]*

[1] Department of Biology, Pennsylvania State University, University Park, PA 16802, USA.
[2] Committee on Evolutionary Biology, University of Chicago, 1027 E 57th St, Chicago, IL 60637, USA.
[3] Department of Organismal Biology and Anatomy, University of Chicago, 1027 E 57th St, Chicago, IL 60637, USA.
*Corresponding author. Email: mcoates@uchicago.edu

ABSTRACT: *Rhadinichthys* is one of the most wide-ranging and speciose genera of Palaeozoic actinopterygians. A classic variety of 'palaeoniscoid', *Rhadinichthys* species are generally small (~10–15 cm) and known mostly from dermal skeletal remains that show features commonplace among early ray-finned fishes. For this reason, the genus has long been considered a poorly diagnosed wastebasket taxon in need of revision and rarely included in systematic analyses. In the present work, syntypes of *Rhadinichthys ornatissimus*, the type species, are re-examined and supplemented with better-preserved material from other localities in the Scottish Midland Valley. A neotype is nominated and a more precise diagnosis presented with a suite of genus-level apomorphies. Unexpectedly, these traits are also evident in the monotypic Lower Carboniferous actinopterygian genus *Woodichthys*, which the neotype of *R. ornatissimus* closely resembles. As a result, the genus *Woodichthys* is subsumed within the redefined *Rhadinichthys*, and the single *Woodichthys* species is reassigned as *R. bearsdeni*, comb. nov., bringing with it a set of endoskeletal data. Some of these data are new, derived from μCT scans of the skull of the *R. bearsdeni* holotype, yielding renderings that update the original description of its skull table, parasphenoid, neurocranium, and otoliths. Further new data concerning the hyoid arch are obtained from a new specimen of *R. bearsdeni* from a site close by the original Bearsden locality. Redefined in this way, *Rhadinichthys* presents a data-rich operational taxonomic unit better suited for systematic studies. However, in so doing, it also releases a cluster of fossil species no longer anchored to a genus and now in need of rediagnoses.

KEY WORDS: Actinopterygii, palaeontology, Scotland, systematics, wastebasket taxa, μCT

Rhadinichthys (Traquair 1877a) is a classic 'wastebasket' genus among Palaeozoic actinopterygians. A succession of diagnoses (Traquair 1877a, 1911; Moy-Thomas & Bradley Dyne 1938; Lund & Poplin 1997; Elliot 2016; Schultze *et al.* 2021) has sustained this nominal group as a repository for indeterminate early ray-finned fishes, because the formulations consist of combinations of generalised features. Currently, *Rhadinichthys* comprises 27 species found across North and South America, Europe, Russia, and South Africa, with temporal occurrences ranging from the Upper Devonian to the early Permian (Schultze *et al.* 2021; Henderson *et al.* 2023, fig. 7g). Given this extraordinary temporal and spatial range, it is unsurprising to find that *Rhadinichthys* species display significant variation in dermal skull composition, dermal skeletal ornamentation, squamation patterns, fin structures, and other features that usually provide the basis for morphologically distinct genera. As a result of this loose taxonomic definition, *Rhadinichthys* is rarely included in evolutionary analyses. Predictably, when it is included, such as in Gardiner & Schaeffer's (1989) exploration of early actinopterygian diversity, the disparate species emerge scattered across three distinct 'terminal groups': the *Australichthys group* (*R. canobiensis*), the *Belichthys group* (*R. carinatus*), and the *Amblypterus group* (*R. ornatissimus*). Moreover, despite 13 species pruned from *Rhadinichthys* in the last century, and further review and evaluation (e.g., Schultze *et al.* 2021), the genus persists as ill-defined and in need of a more phylogenetically structured treatment.

The type species, *Rhadinichthys ornatissimus*, was first described by Agassiz (1835) and named *Palaeoniscus ornatissimum*. Subsequently, Traquair (1877a) reclassified *P. ornatissimum* as *Rhadinichthys lepturus*, and designated two of the three specimens employed in Agassiz's description as syntypes: NMS G.1896.147.1 and NMS G.1878.18.7 (Fig. 1a, b). Some three decades later, Traquair (1911) revised the species to *Rhadinichthys ornatissimus* and officially assigned it as the genus type. However, from the outset he expressed concern about the condition of the species (and genus) type specimens, noting that 'they are in a very bad state of preservation' (Traquair 1911). Significantly, Traquair's updated description figured other material (e.g., NMS G.1859.33.66, Traquair 1909, fig. 2, pl. XXVIII), and relied on these for much of the morphological detail. Currently, both syntypes NMS G.1896.147.1 and NMS G.1878.18.7 appear to have

 doi:10.1017/S1755691024000136

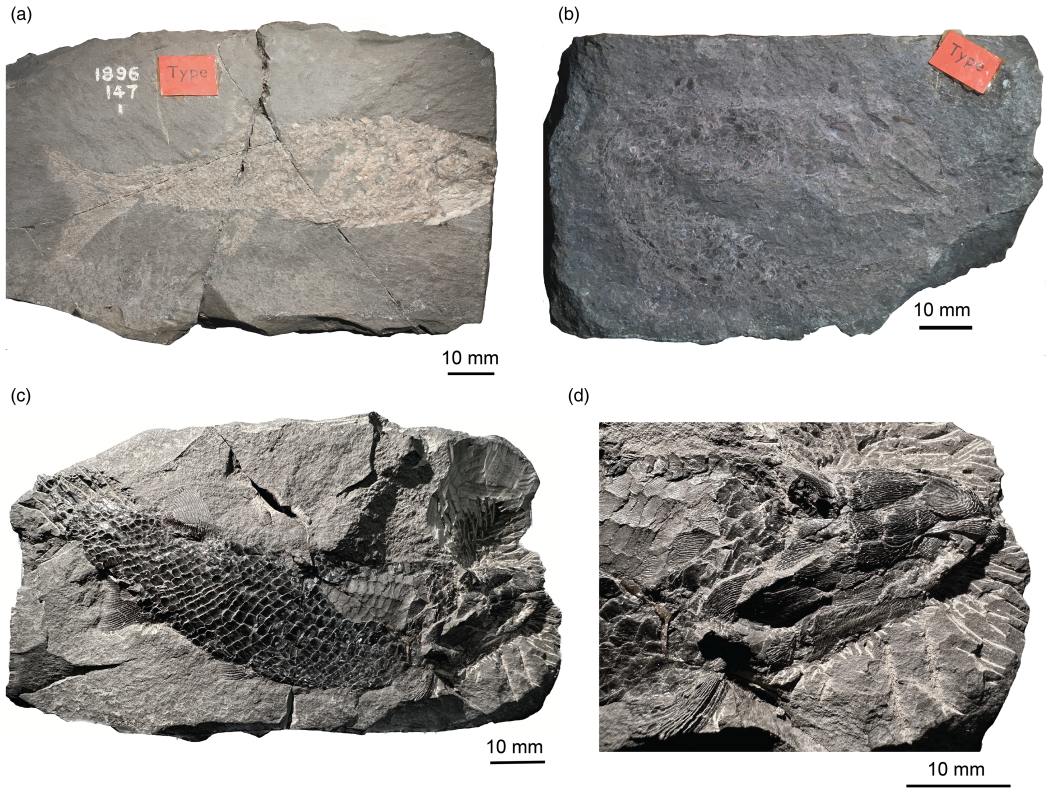

Figure 1 Types of *Rhadinichthys ornatissimus*. (a) Original syntype of *Rhadinichthys ornatissimus*, NMS G.1896.147.1. (b) Original syntype of *Rhadinichthys ornatissimus*, NMS G.1878.18.7. (c) Proposed neotype for *Rhadinichthys ornatissimus*, NMS G.1891.24.11. (d) Close-up on the cranium of NMS G.1891.24.11.

undergone further wear and tear, and, in agreement with other researchers (Giles *et al*. 2023), two of the present authors (pers. obs., AMC and MIC) consider few of the remaining features as usable for diagnosis (see Fig. 1a, b). For this reason, a further specimen, NMS G.1891.24.11 (Fig. 1c, d) is offered as a neotype because it more clearly displays the specialised traits that might be used as distinctive characteristics at species and genus levels.

Although *Rhadinichthys* forms the focus of this study, the project started out rather differently. The initial aim was to update the description of the Lower Carboniferous taxon *Woodichthys bearsdeni* (Coates 1998), adding data from µCT scans of the holotype skull table and neurocranium NMS G.1984.42.15 (Fig. 2), and data now available from a previously undocumented specimen, GLAHM 163425a and b (Figs 3, 4). First described by Coates (1998), *Woodichthys bearsdeni* is one of only a handful of Carboniferous actinopterygians with an at least partly described braincase (cf. review in Caron *et al*. 2023), and for this reason the species has been included in several phylogenetic analyses over the past 25 years (Coates 1999; Cloutier & Arratia 2004; Giles *et al*. 2017, 2023). However, renewed comparison with *Rhadinichthys ornatissimus*, and especially with the proposed neotype, revealed a series of shared specialisations, thereby driving the study in an unexpected direction. With a sister-species relationship between *R. ornatissimus* and *W. bearsdeni* evident, this work now also evaluates the possibility of subsuming the monospecific genus *Woodichthys* within *Rhadinichthys*, refines the definition of *Rhadinichthys*, and reassesses the current membership of the genus. Through these systematic revisions, the intention of this study is to re-establish *Rhadinichthys* as an informative taxonomic unit that will contribute to a better understanding of early actinopterygian diversity and interrelationships.

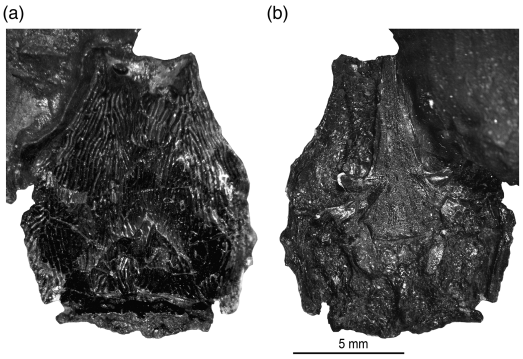

Figure 2 *Rhadinichthys bearsdeni*, comb. nov. (formerly *Woodichthys*), microscope images of holotype braincase NMS G.1984.42.15c in dorsal (a) and ventral (b) views.

Terminology for cranial bones in the present work follows the standard nomenclature used in monographic studies of comparable taxa; most notably Gardiner's (1984) descriptions of *Mimipiscis* and *Moythomasia*. Other naming schemes are available, acknowledging the well-corroborated homology of actinopterygian frontals with sarcopterygian parietals, and actinopterygian parietals with sarcopterygian postparietals. For an efficient summary of alternative terminologies

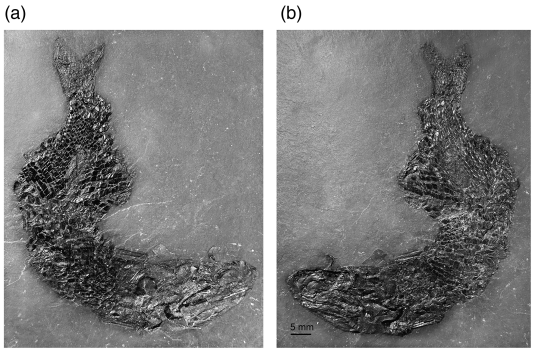

Figure 3 *Rhadinichthys bearsdeni,* comb. nov. (formerly *Woodichthys*), photographs of GLAHM 163425a and b: (a) part; (b) counterpart.

and equivalents see Pearson & Westoll (1979, table 1). For a lengthier discussion, including compound names for single bones where they are inferred to be the product of ancestrally distinct bones, see Schultze *et al*. (2021). Here, the aim is to provide descriptions using terms that will assist placement of *Woodichthys* and *Rhadinichthys* among the Actinopterygii.

Finally, this paper is contributed to celebrate the work of Tim Smithson. His studies of early vertebrates, and especially of early tetrapods and lungfish, built on a sustained and productive scouring of the Scottish Borders for lost and new fossil localities, have been outstanding and transformative. One of us (MIC) was fortunate enough to overlap with Tim's presence in Alec Panchen's research group at The University of Newcastle Upon Tyne. The benefits of Tim's advice and informal mentorship were more than significant. This offering is, we hope, a fitting tribute.

1. Materials

1.1. Image preparation

Fossil specimens were scanned at the University of Chicago X-ray µCT facility on a GE Phoenix 240/180 scanner using the 240 microfocus tube. Specimen NMS G.1984.42.15.c was scanned with 70 kv, 100 mA, no filter, 2,000 projections, 500 ms timing, and voxel size of 9.52 µm. Specimens GLAHM 163425a and b were scanned using 120 kv, 140 mA, 0.1 mm copper filter, 2,000 projections, 500 ms timing, and voxel size of 23.4 µm. Tomographic image stacks are available for download on Morphosource. Segmentation and anatomical reconstruction were accomplished using Materialise Mimics v.25 (biomedical.materialise.com/mimics; Materialise 2016, Leuven, Belgium). Imaging of digital models was completed using Blender 3.2

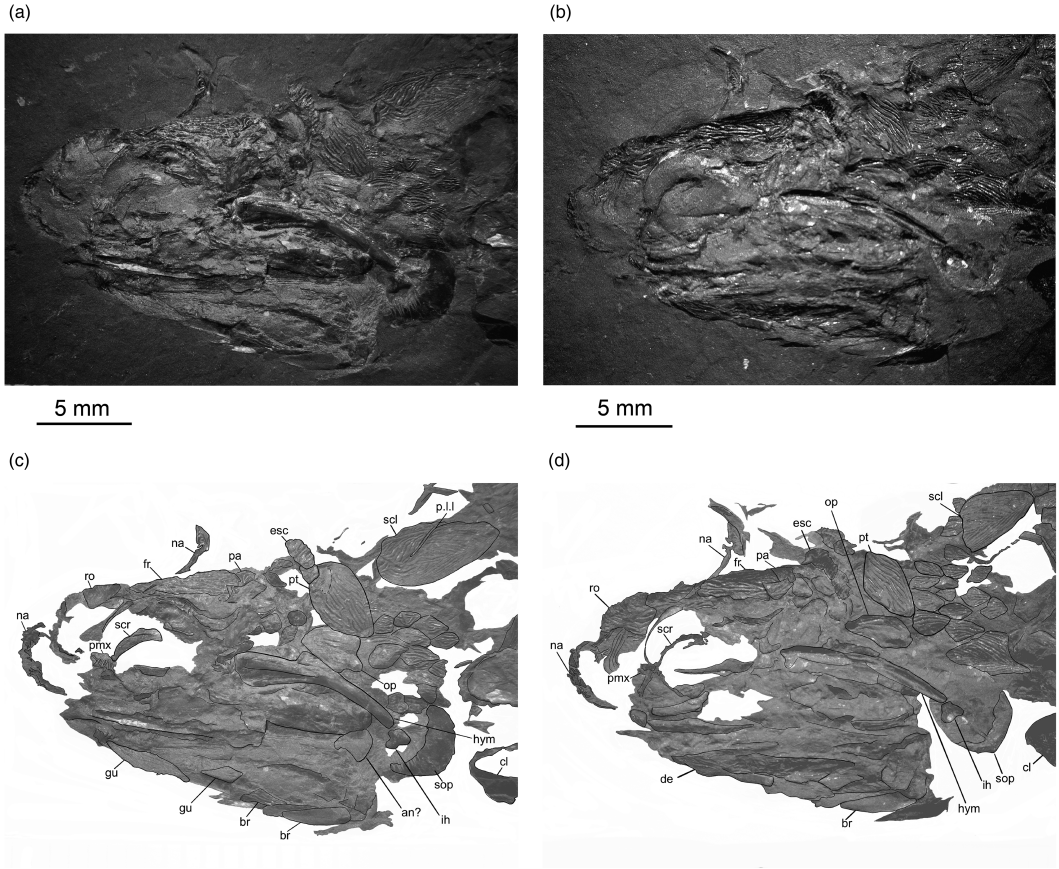

Figure 4 *Rhadinichthys bearsdeni,* comb. nov. (formerly *Woodichthys*), close-up on the cranial portion of GLAHM 163425a and b. See Fig. 15 for µCT 3D reconstruction of the same specimen. (a, c) GLAHM 163425a. (b, d) GLAHM 163425b, image reversed for ease of comparison between part and counterpart. (a, c) photographs of specimen. (b, d) Inked diagram. Abbreviations: an = angular; br = branchiostegal plates; cl = cleithrum, de = dentary; esc = extrascapular; fr = frontal; gu = gular; hym = hyomandibula; ih = interhyal; na = nasal; op = operculum; pa = parietal; p.l.l = posterior lateral line; pt = posttemporal; ro = rostral; scl = supracleithrum; scr = sclerotic ring; sop = suboperculum.

(Community 2018). Photography of fossil specimens was accomplished using a Leica DFC490 camera attached to a Zeiss Stemi SV6 microscope processed in Image-Pro Plus 6.2 using the enhanced depth of field function, and an iPhone 14 Pro rear camera.

1.2. Abbreviations

1.2.1. Institutional abbreviations. NMS, National Museums Scotland, Edinburgh; GLAHM, Glasgow University, Hunterian Museum, Glasgow; MCZ, Harvard University Museum of Comparative Zoology, Cambridge, Massachusetts, USA.

1.3. Specimens and geological context

The type specimens of *Rhadinichthys ornatissimus*, NMS G.1896.147.1 and NMS G.1878.18.7, were examined and photographed at the National Museums Scotland. NMS G.1896.147.1 (Fig. 1a) is from the Strathclyde Group (formerly known as the Calciferous Sandstone Series) at Burntisland, Fife (Firth of Forth north shore). The rostral part of the head is missing but body and median fin outlines are near complete. This specimen is in poor condition and of less diagnostic value than the other. NMS G.1878.18.7 (Fig. 1b) is from the Carboniferous limestone bed of Burdiehouse about four miles south of Edinburgh. The body is near complete although jack-knifed at the level of dorsal and anal fins (the same contortion evident in other Burdiehouse specimens, e.g., NMS G.1859.33.66). Exposed surfaces are partly eroded but retain surface ornament and the skull table is in fair condition. The proposed neotype of *Rhadinichthys ornatissimus*, NMS G.1891.24.11 (Fig. 1c, d), is from Straiton Oil Shale Works (about two miles south of Burdiehouse), from the roof of the Dunnet Shale, deposited during Asbian to Brigantian substages of the Carboniferous period, ~335.59–328.48 Ma BP (Aretz *et al.* 2020). NMS G.1889.115.3, a further whole-body specimen including a reasonably complete cranium, is also from the Straiton Oil Shale Works. Burdiehouse specimen NMS G.1859.33.66.1 and 2, part and counterpart, mentioned above, is a Hugh Miller specimen, with a fileted cranium and a splayed, well-preserved, pectoral fin. MCZ 10620 is from the Wardie Shales member of the Gullane Formation exposed at Granton Harbour, Edinburgh, and dates from ~331.1–335.5 Ma BP (Monoghan *et al.* 2014; Friedman *et al.* 2018; Aretz *et al.* 2020). The specimen, part of the Thomas Stock collection, consists of the anterior third of a fish and exhibits some rostro-caudal compression; surface detail is poor.

All the specimens of *Woodichthys bearsdeni* here examined are from the Manse Burn Formation: fine marine shales ranging from the Top Hosie Limestone Marine Band down to the first thick sandstone and dated to the Pendleian (~330.34–327 Ma BP, substage of the Serpukhovian) E1 Zone of the Lower Carboniferous (Clark 1989; Aretz *et al.* 2020). NMS G.1984.42.15.c includes the dorsoventrally flattened braincase of the *Woodichthys bearsdeni* holotype (Fig. 2), which was collected from the Bearsden exposure of the Manse Burn Formation (Wood 1982). The first description of NMS G.1984.42.15.c included camera lucida drawings of the dorsal and the incomplete ventral surface, and a radiograph revealing a portion of the right supraorbital canal (Coates 1998). GLAHM 163425a and b (Figs 3, 4) were collected by Mr. P. Gavin from a further exposure of the Manse Burn Formation in Faifley, Clydebank, approximately two miles southwest of the Bearsden locality. This full-body specimen contains a well-preserved hyoid arch that has not been documented for *R. bearsdeni* in previous literature. Both individuals are slightly pyritised and significantly compacted, and both preserve three-dimensional otoliths.

Source localities of all referred specimens are mapped in Fig. 5.

2. Systematic palaeontology

Osteichthyes Huxley 1880
Actinopterygii Woodward 1891
Incertae sedis Genus *Rhadinichthys* Traquair 1877a.

Synonymy. *Rhadinichthys* (Traquair), Moy-Thomas & Bradley Dyne (1938, p. 450).

'Rhadinichthyids group', Lund & Poplin (1997, p. 483).
Rhadinichthys (Traquair), Elliott (2016, p. 356).
Rhadinichthys (Traquair), Schultze *et al.* (2021, p. 129).

Type species. *Rhadinichthys ornatissimus* Traquair 1877a.

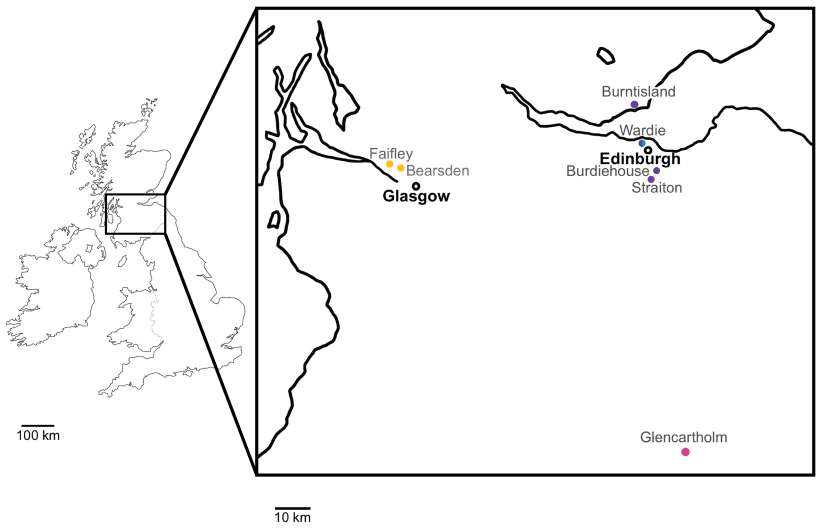

Figure 5 Collection localities of the redefined *Rhadinichthys* species: *Rhadinichthys bearsdeni* comb. nov. (formerly *Woodichthys*), (yellow: Faifley and Bearsden), *Rhadinichthys ornatissimus* (purple: Burntisland, Wardie, Burdiehouse, and Straiton), *Rhadinichthys ferox* (turquoise: Wardie), *Rhadinichthys laevis* (pink: Glencartholm).

Emended generic diagnosis. Fusiform body with total length ranging from 10 to 15 cm; skull roof, cheek and lower jaw ornament of fine, anteroposteriorly aligned, closely packed elongate ridges. Frontal more than twice parietal length; parietals less than two thirds of frontal width. Supratemporal with broad, medially expanded posterior portion and short anterior limb; thus, full width of skull table rear with near equal contribution from supratemporal and parietal; intertemporal narrow. Rostral with low apex and subrectangular broad midline plate with straight posterior margin; rostral ornament transitions from pitted enamel snout-cap to ridge-on-plate posteriorly; nasal notch preceded by ornament-free margin. Premaxillae broad and sub-pentagonal; suborbitals absent; opercular more than twice subopercular height; branchiostegals numerous. Scales arranged in 36+ precaudal rows; scales serrated posteriorly; scales close to dorsal midline and anterior flank bear fine ridged ornament; lateral line scales pierced occasionally by large slot-shaped pores; three basal fulcra, of which the largest bears a pair of slot-shaped pores, precede dorsal fin. All fins with fringing fulcra; pectoral lepidotrichia unsegmented proximally; all median fins in rear half of body; dorsal fin opposite or precedes level of anal fin.

Type species. *Rhadinichthys ornatissimus* (Traquair 1911).

Synonymy. *Palaeoniscus ornatissimus* Agassiz (1835, p. 92).

Rhadinichthys lepturus Traquair (1877a, p. 437).

Emended species diagnosis. *Rhadinichthys* with total length of approximately 12–15 cm; frontal with rounded posterolateral extremity; parietal subrectangular; rostral apex pitted with short grooves; pores of anterior lateral lines large on nasal and supratemporal; opercular bone covered in fine ridged ornament. Scale rows with eight or more members above and six or more below the lateral line in flank region; scale ornament with fine horizontal ridges across entire dorsal surface; scales on posterior and ventral parts of body generally smooth. Dorsal fin only slightly anterior to level of anal fin; pair of basal fulcral scales precede anal fin.

Syntypes. NMS G.1878.18.7, NMS G.1896.147.1.

Proposed neotype. NMS G.1891.24.11.

Referred specimens and localities. NMS G.1878.18.7 and NMS G.1859.33.66, part and counterpart, Carboniferous limestone, Burdiehouse, Edinburgh; MCZ 10620, Wardie Shales, Granton, Edinburgh; NMS G.1896.147.1, Strathclyde Group, Burntisland, Fife; NMS G.1891.24.11 and NMS G.1889.115.3, Dunnet Shale, Straiton, Midlothian.

Species. *Rhadinichthys bearsdeni* comb. nov.

Synonymy. *Woodichthys bearsdeni* Coates (1998, pp. 37–38).

Emended species diagnosis. *Rhadinichthys* with total length of around 11 cm; frontal with angled posterolateral extremity; parietal span narrow, meeting less than half of frontal posterior margin; parietal with narrow anterior process projecting into rear of frontal. Rostral apex ornamented with pits; nasal enclosed supraorbital canal with short posterior rami; jugal enclosed infraorbital canal with posterior rami; opercular and subopercular plate fine-ridged ornament diminishes posteriorly and ventrally, away from anterior and dorsal margins. Scale rows with ten or more members above and six or more below the lateral line in flank region; scale ornament maximal in nape region, flank scale surfaces mostly smooth, with slight ornament of parallel grooves across anterodorsal region. Dorsal fin mostly anterior to level of anal fin; single basal fulcral scale precedes caudal and anal fins.

Holotype. NMS G.1984.42.15.a, b, and c.

Referred specimens and localities. NMS G.1983.33.2, NMS G.1984.42.15.c, and NMS G.1987.7.133 from Manse Burn Formation, Bearsden, Glasgow; GLAHM 163425a and b from Manse Burn Formation, Faifley, Glasgow.

3. Results

3.1. Description of *Rhadinichthys ornatissimus*

3.1.1. Head. Details of the cranium are taken mostly from specimens NMS G.1891.24.11 (the neotype) (Figs 6c–8a) and NMS G.1889.115.3, with corroboration from type specimen NMS G.1878.18.7. In general, cranial morphology closely resembles that of *R. bearsdeni* comb. nov. (Coates 1998). The general arrangement, proportions, and dermal ornament of posttemporal, parietal, frontal, supratemporal, and intertemporal, are shared in both species. Notably, the supratemporal (st, Fig. 8a) is unusually broad posteriorly, like that of the redescribed skull table of NMS G.1984.42.15.c (Fig. 9). In both examples a deeply recessed anteromedial accommodates the posterolateral angle of the frontal. The extrascapulars are not well preserved in *R. ornatissimus*. Details of this skull table arrangement are also visible in natural mould on the type specimen NMS G.1878.18.7. The large rostral (ro, Figs 6c, 8a) has a broad posterior plate ornamented with ridges aligned with the lateral margins, but these ridges curve medially and coalesce dorsal to the apex of the snout so that the apex is mostly ganoine-capped, pockmarked with pits and short curved grooves, unlike the central area of posterior plate which is mostly ornament-free. Notches for left and right anterior nostrils flank the snout apex, and these notches are preceded by a marked ornament-free margin.

The nasal bone (na, Figs 6c, 8a) of NMS G.1891.24.11 resembles the slender proportions of that seen in *Rhadinichthys bearsdeni* comb. nov. (Fig. 4), but bears a series of pores overlying the sensory canal. Similarly sized pores are visible on portions of the skull table, also tracking the cranial lateral lines. Such easily identified pores are not evident in *R. bearsdeni*. A slender, triangular bone lateral to the skull table, projecting into the orbit roof and underlying the nasal, appears to be a displaced dermosphenotic. The maxilla is incompletely preserved in NMS G.1889.115.3 and 1891.24.11; enough of the posterior portion is preserved to indicate that the gross morphology and ornament of dorsally and anteriorly swept ridges resembles that of *R. bearsdeni* comb. nov. (mx, Fig. 8a, b). The anterior portion of the preopercular is preserved dorsal to the posterior part of the maxilla in NMS G.1891.24.11. Importantly, the ornament shows the distinctive change in pattern between dorsal and ventral areas of the bone (compare examples in Fig. 8a, b). Dorsally, ornament ridges are vertically oriented, anteriorly concave crescents; ventrally, ridges are horizontal, near straight, and parallel to the ventral margin. There are no notches in the preopercular margin or small isolated plates indicating the presence of suborbital bones. The opercular bones of NMS G.1891.24.11 and 1889.115.3 resemble those of *R. bearsdeni*, but with a more complete covering of finely ridged ornament. In both bones the ornament radiates from the anterodorsal corner of the plate.

3.1.2. Fins. All fins, except the pectoral, are situated at the rear half of the body. The pectoral fin inserts posterior to the cranium and comprises a minimum of 20 unsegmented lepidotrichia (Fig. 6e). A splayed pectoral fin, revealing the complete, broad, triangular outline, is preserved in the Burdiehouse specimen NMS G.1859.33.66. Although clearly depicted by Traquair (1909, pl. 28, fig. 2), this illustration trims the extremities; the greatest extent of the fin (although not preserved in high resolution) is proportionally equal to the length of the maxilla. The pectoral fin is not 'rather small', contra Traquair (1911). The proximal, elongate segments of the lepidotrichia account for just over half of the total length of the principal fin rays. Fringing fulcra are small and adhere tightly to the leading edge. The pelvic fin is positioned at the midpoint between the pectoral and anal fins, and contains minimally 14 short fin rays, the principal rays segmenting five or six times and bifurcating distally (Fig. 6f). Fringing fulcra are present.

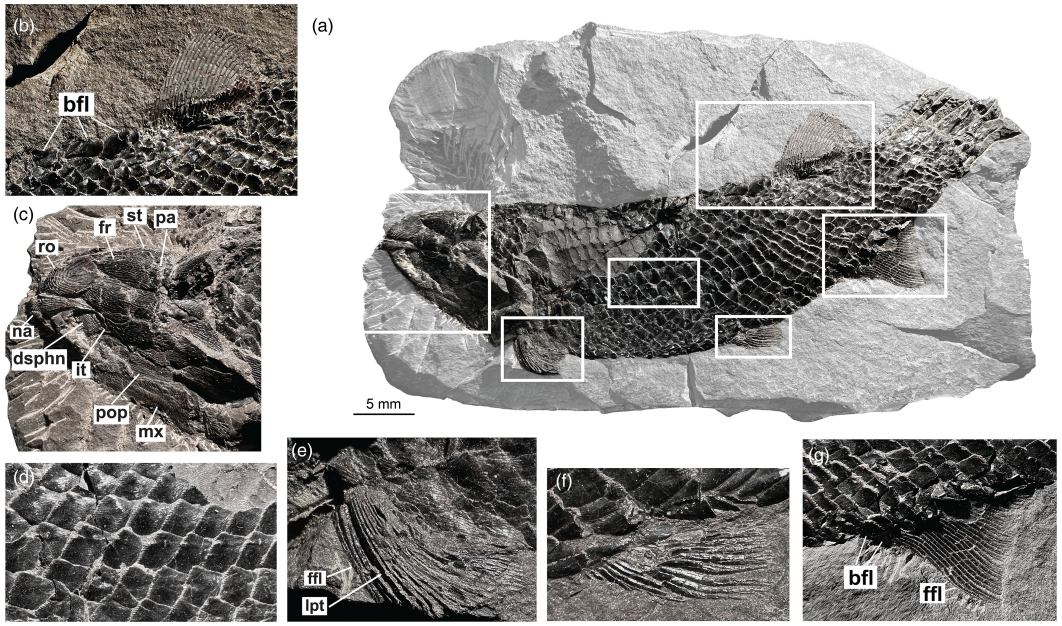

Figure 6 *Rhadinichthys ornatissimus*, photograph of NMS G.1891.24.11 with close-ups of notable features. (a) Full specimen. (b) Dorsal fin and basal fulcral scales. (c) Dorsoventrally compressed cranium. (d) Lateral line scales and pores. (e) Pectoral fin with unsegmented lepidotrichia. (f) Pelvic fin. (g) Anal fin. Abbreviations: bfl = basal fulcra; dsphn = dermosphenotic; ffl = fringing fulcra; fr = frontal; it = intertemporal; lpt = lepidotrichia; mx = maxilla; na = nasal; pa = parietal; pop = preoperculum; ro = rostral; st = supratemporal.

The dorsal fin (Fig. 6b) is triangular and has 25 slender lepidotrichia which can segment up to eight times. No fringing fulcra are preserved, but they are probably lost; preservation is mostly mouldic. The anal fin (Fig. 6g) in NMS G.1891.24.11 is well preserved. Located almost dorsoventrally level with the dorsal, it consists of similar numbers of lepidotrichia. Each fin ray segments from four to eight times and bifurcates distally. At the first and subsequent bifurcations the anterior branch is consistently thinner than the posterior branch, which bifurcates

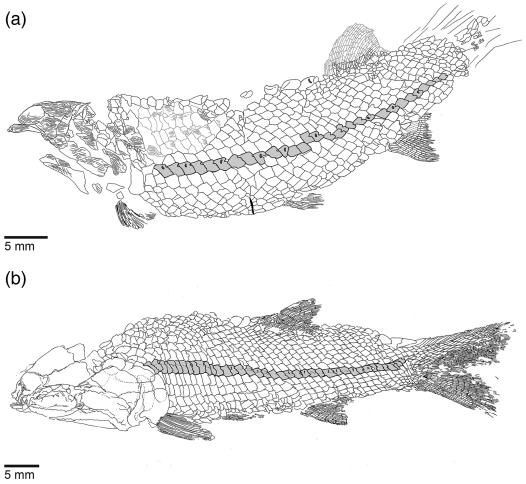

Figure 7 Line drawings of *Rhadinichthys ornatissimus* and *Rhadinichthys bearsdeni* comb. nov. (formerly *Woodichthys*). (a) *R. ornatissimus* NMS G.1891.24.11, specimen map with lateral line scales shaded grey. (b) *R. bearsdeni* NMS G.1983.33.2 specimen map with lateral line scales shaded grey (adapted from Coates 1998, fig. 10a; reversed for direct comparison).

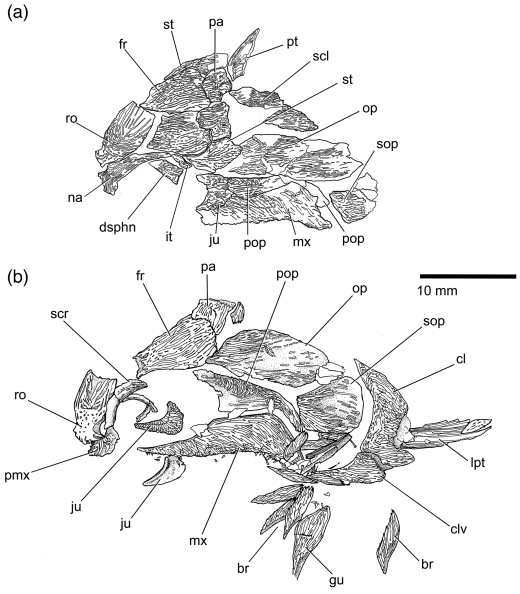

Figure 8 *Rhadinichthys ornatissimus* and *Rhadinichthys bearsdeni* comb. nov. (formerly *Woodichthys*): associated dermal cranial bones in external view. (a) *R. ornatissimus* NMS G.1891.24.11. (b) *R. bearsdeni*. NMS G.1987.7.133 specimen map with lateral line scales shaded grey (adapted from Coates 1988, fig. 9 and 1998, fig. 7a). Abbreviations: br = branchiostegal plate; clv = clavicle; dsphn = dermosphenotic; fr = frontal; gu = gular; it = intertemporal; ju = jugal; lpt = lepidotrichia; mx = maxilla; na = nasal; op = operculum; pa = parietal; pmx = premaxilla; pop = preoperculum; pt = post temporal; ro = rostral; scl = supracleithrum; scr = sclerotic ring; sop = suboperculum; st = supratemporal.

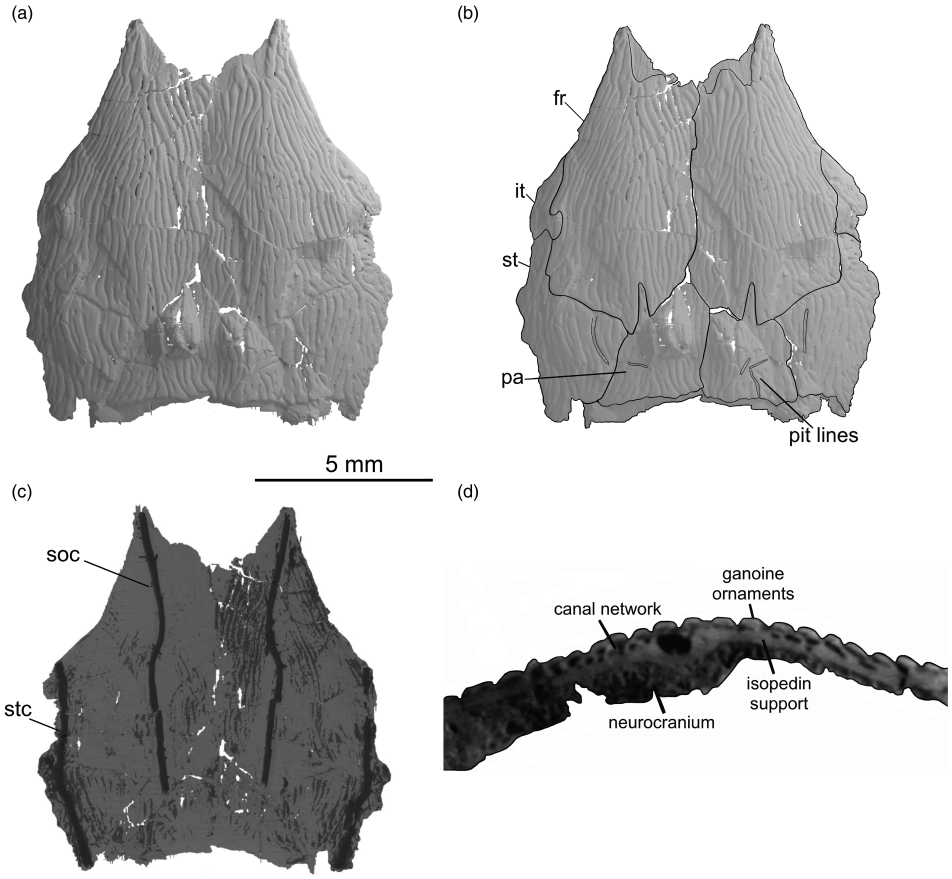

Figure 9 *Rhadinichthys bearsdeni* comb. nov. (formerly *Woodichthys*), NMS G.1984.42.15.c skull table. (a) μCT 3D reconstruction of the skull table, dorsal view. (b) Inked diagram illustrating dermal sutures, dorsal view. (c) Skull table made transparent to reveal the supraorbital and otic canals, ventral view. (d) Tomographic slice revealing histological structures of the dermal skull table, sagittal view. Abbreviations: fr = frontal; it = intertemporal; pa = parietal; soc = supraorbital canal; st = supratemporal; stc = supratemporal canal.

again, distally (the anterior branch no longer bifurcates). This asymmetry in branching pattern appears to be present in the dorsal fin too, but evidence from the matrix mould is less clear. Both fins are broad-based, spanning eight or nine scale rows in contrast to three for the pelvic fin.

The caudal fin is not well preserved in any specimen examined. The most complete example observed is in NMS G.1889.115.3, in which it resembles conditions in *R. bearsdeni* comb. nov.

3.1.3. Squamation. The flank scales of *Rhadinichthys ornatissimus* are rhomboid and serrated posteriorly (12–15 serrations, depending on scale shape). The exposed surface of each scale bears fine ridges, and with low angle lighting these can be seen to extend across much of each scale's surface. The ornament is most prominent towards the anterodorsal process, from which the ridges mostly extend. There is slight regional variation in ornamentation across the body, with smoother surfaces posteriorly and ventrally. The squamation consists of at least 36 obliquely oriented, precaudal scale rows, with each row containing eight or more scales above and six or more scales below the lateral line (Figs 6d, 7a). Towards the dorsal and ventral midlines, the scales become dorsoventrally shallower, but the scale rows show no marked subdivisions into fields of smaller units. Scale length is mostly uniform. As in *Rhadinichthys bearsdeni* comb. nov., the lateral line can be easily traced by specialised canal-carrying scales, occasional members of which are pierced by slot-shaped pores (Figs 6d, 7a) and distinct notches in the trailing edge. Both the dorsal and the anal fins are preceded by enlarge fulcral scales (Fig. 6b, g). Three fulcral scales are present in front of the dorsal fin, and a pair of pores is present on the largest of the series. A pair of fulcra scales lies anterior to the anal fin.

3.2. Redescription of NMS 1984.42.15.c, *Rhadinichthys bearsdeni* comb. nov.

The following description refers to those parts of the material re-examined as part of the present project; further details of the skeletal anatomy are provided in the original report (Coates 1998).

3.2.1. Skull table. The preserved skull roof (Figs 2a, 8b, 9) includes the paired frontals, parietals, intertemporals, and supratemporals. Dermal sutural patterns were determined from visible overlaps between each bone in cross-sectional views in the tomograms, and the shape of the supratemporal, especially, and its adjacent parietal were revised accordingly (compare visible morphology and μCT scan renderings in Figs 2a and 9b). The shape of the frontal (Fig. 9b) is as described in Coates (1998) and closely resembles that of *Rhadinichthys ornatissimus*. However, reassessment of the dermal sutures has decreased the lateral extent of the parietal by at least 25 %. After revision, the parietal maximum width measures approximately 60 % of the frontal in maximum width and 30 % in length, a proportion

resembling the short and narrow parietal of *Pteronisculus* (Nielsen 1942). Left and right parietals (Fig. 9b) are notably asymmetric, with the left parietal slightly larger in size and suturing in part with the right frontal. Both parietals bear a narrow, acute process, unnoticed in the original description, protruding from the anterior edge and enclosing the posterior-most portion of the supraorbital canal. Three convergent pit lines lie in the posterior centre of the right parietal. Identifying pit lines on the left side proves challenging, since it was more severely fractured by the otoliths punching through during taphonomic compression. Only one unambiguous pit line is found on the left parietal. At the rear border, a broad, unornamented flange underlies the preceding extrascapular series.

Paths of the paired supraorbital and otic canals are revealed through μCT scanning. The condition of the supraorbital canal (Fig. 9c) bears strong similarity to *Phoebeannaia* (Caron *et al.* 2023, figs 5a, 9b). In both taxa, it enters the dermal skull from the narrow anterolateral extremity of the frontal, then travels along the frontal midline and through the anterior process of the parietal, terminating just posterior to the process. The canal does not follow a straight course but kinks laterally around its midpoint. Of possible phylogenetic significance, this kink is absent in Devonian taxa such as *Mimipiscis* (Gardiner 1984, fig. 80) and *Raynerius* (Giles *et al.* 2015). Short, twig-like offshoots emerge sparsely along the anterior half of the canal in *Rhadinichthys bearsdeni*. These twigs either reach upward to the dorsal exterior or penetrate ventrally through the lowest layer of the dermal bone and into the compressed braincase. External pores marking the track of the line through the frontal are difficult to locate, and the path of the canal is not especially evident in the pattern or 'fingerprint' of dermal ornament. The otic extension of the main lateral line canal (Fig. 9c) runs close to the lateral edge of the supratemporal, as shown by Coates (1998, fig. 8b).

The intertemporal (Fig. 9b) is short and near rhombic as originally described. The revised supratemporal (Fig. 9b) is narrow where it flanks the frontal, but then broadens towards the dorsal midline following the contour of the frontal and sharply notches into the frontal-parietal series. This posterior expansion of the supratemporal occupies 50 % of the posterior rim of the frontal. The unusual shape (broad posterior plate with short and narrow anterolateral limb) is distinctively similar to that present in *Rhadinichthys ornatissimus* (compare examples in Figs 8a and 9b). A deep groove is visible near the junction of the supratemporal, frontal, and parietal bones, possibly representing an additional pit line.

Histological structure of the dermal bone was also captured by the μCT scan, albeit in low resolution. The dermal bone consists of three distinct layers: an uppermost layer of ganoine-covered ornament, a middle layer with a canal network, extending both dorsally and ventrally for passages of nerves and vessels, and a compact basal layer (Fig. 9d). The dermal ornament is clearly displayed in the three-dimensional rendering of the skull roof (Fig. 9a): ganoine ridges align anteroposteriorly, following the longitudinal direction of each skull bone (consistent with line illustration in Coates 1998). This unidirectional pattern is consistent with that of *Rhadinichthys ornatissimus*.

3.2.2. Parasphenoid. The parasphenoid (Figs 2b, 10–12a–c) tapers rostrally and possesses an anteriorly directed dermal basipterygoid process as well as a broad, proximodistally short ascending process. Morphologically, the parasphenoid resembles that of *Kansasiella* (Poplin 1974, 1975; Caron *et al.* 2023). Posteriorly, the parasphenoid reaches the ventral otic fissure but does not extend across it. A buccohypophyseal canal pierces the external (ventral) surface level with the anterior margin of the basipterygoid process. The canal extends posterodorsally at a

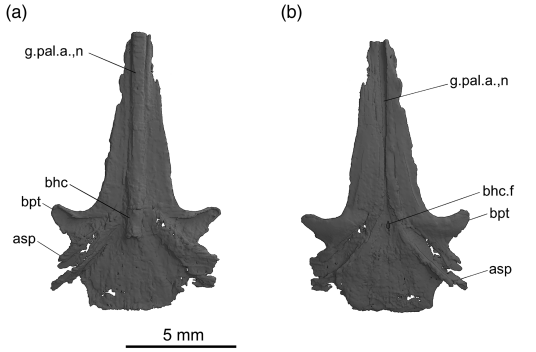

Figure 10 *Rhadinichthys bearsdeni* comb. nov. (formerly *Woodichthys*), NMS G.1984.42.15.c parasphenoid in dorsal (a) and ventral (b) views. Abbreviations: asp = ascending process; bhc = buccohypophyseal canal; bhc.f = foramen for buccohypophyseal canal; bpt = basipterygoid process; g.pal.a.,n = groove for the palatine artery and nerve.

20-degree angle (Fig. 11a) and terminates at the internal (dorsal) surface level with the posterior of the basipterygoid process.

A denticle field, visible on the actual specimen and in specimen photographs (Figs 2b, 11b) but barely discernible in μCT slices, occupies the central, buccal, parasphenoid surface, including the posterior expanded region and the spiracular grooves of the ascending process. In the denticle-free peripheral regions, thin and compact striations ornamented the exposed areas. The ascending process is broad but short; its lateral extent does not exceed that of the basipterygoid process (although slightly longer

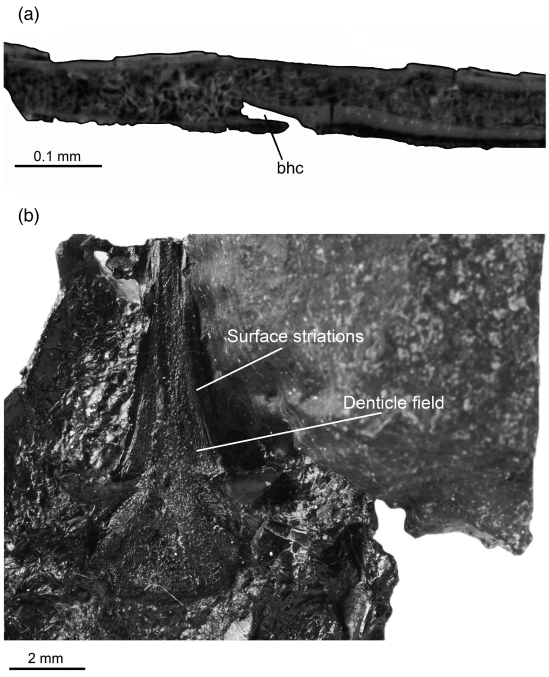

Figure 11 *Rhadinichthys bearsdeni* comb. nov. (formerly *Woodichthys*), NMS G.1984.42.15.c, additional details of parasphenoid anatomy. (a) Microtomographic cross-section showing the path of the buccohypophyseal canal, sagittal view. (b) Close-up of the ventral exposed surface of the parasphenoid from a specimen photo. The denticle field, as well as thin striations lateral to the denticle field, are visible from the photograph. Abbreviation: bhc = buccohypophyseal canal.

than reconstructed by Coates 1998). Thus, unlike Carboniferous actinopterygians such as *Kansasiella* (Poplin 1974) and *Lawrenciella* (Hamel & Poplin 2008; Pradel *et al*. 2016), the ascending process terminates far short of the spiracular canal.

3.2.3. Neurocranium. The neurocranium (Figs 12, 13) has a maximum length of 15 mm from the broken autopalatine articulation to the posterior of the occiput, and a maximum width of 12 mm across the postorbital processes. Most of its dorsoventral height was lost in postmortem compression. The flattened remains are preserved under the complete skull roof. The ethmoid region is incomplete because of delicate ossification and loss during preparation (Coates 1998).

Details of the orbit are largely obscured, so conditions of the postorbital wall, the trigeminofacialis chamber, and myodomes, if present, remain unknown. The original description (Coates 1998) reported an ossified interorbital septum on the specimen but μCT scans show no strong evidence of its presence, and the previously identified material is the orbit endoskeletal roof. Similarly, a foramen for the efferent pseudobranchial artery was identified at the base of the basipterygoid process (Coates 1998), but successive rounds of three-dimensional reconstruction show no such feature. Frustratingly, some details evident in the original description and on the surface of the actual fossil are barely discernible in the rendering of the μCT data (Fig. 12a). However, slight rotation of the rendering (Fig. 12b) with the otoliths removed reveals significantly more detail, and these data can be augmented by reference to slices from the μCT stack (Fig. 13).

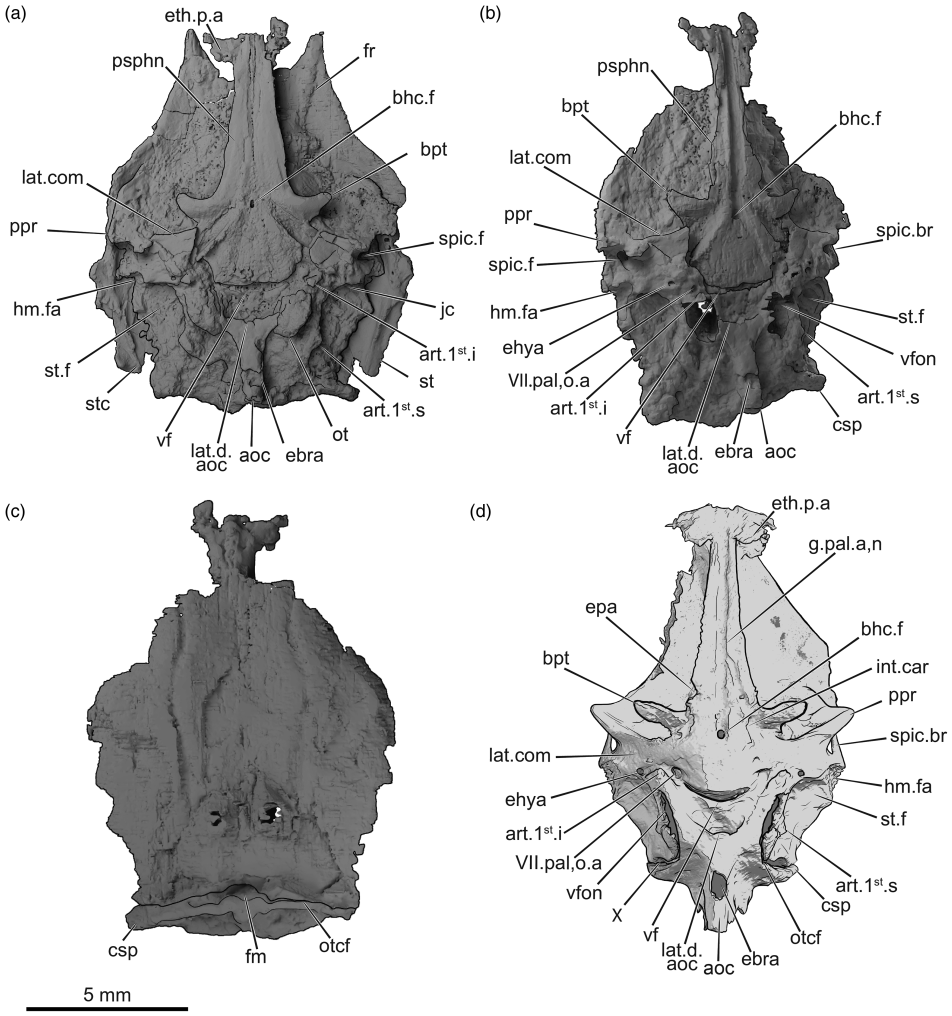

Figure 12 *Rhadinichthys bearsdeni* comb. nov. (formerly *Woodichthys*), neurocranium reconstruction from μCT data of NMS G.1984.42.15.c and comparison with *Phoebeannaia mossae*. (a) Ventral view. (b) Ventral view with the dermatocranium and the otoliths removed, tilted to reveal the vestibular fontanelle and more three-dimensional details of the endocranium. (c) Dorsal view with the dermatocranium removed. (d) Neurocranium of *Phoebeannaia mossae*, adapted from Caron *et al*. (2023). Abbreviations: aoc = aortic canal; art. 1st.i = articulation for infrapharyngobranchial of first gill arch; art. 1st.s = articulation for suprapharyngobranchial of first gill arch; bhc.f = foramen for buccohypophyseal canal; bpt = basipterygoid process; csp = craniospinal process; ebra = canal or foramen for the efferent branchial artery; ehya = canal or foramen for the efferent hyoid artery; ep.a = canal or foramen for the efferent pseudobranchial arteries; eth.p.a = ethmoid articulation for the palatoquadrate; fm = foramen magnum; fr = frontal; g.pal.a, n = groove for the palatine artery and nerve; hm.fa = facet for the hyomandibula; int.car = canal or foramen for the internal carotid; jc = jugal canal; lat.com = lateral commissure; lat.d.aoc = lateral dorsal aortic canal; ot = otolith; otcf = oticooccipital fissure; ppr = postorbital process; psphn = parasphenoid; spic.br = spiracular bridge; spic.f = foramen for spiracular canal; st = supratemporal; stc = supratemporal canal; st.f = subtemporal fossa; VII.pal,o.a = canal or foramen for the palatine nerve and/or orbital artery; vf = ventral fissure; X = canal or foramen for the vagus nerve.

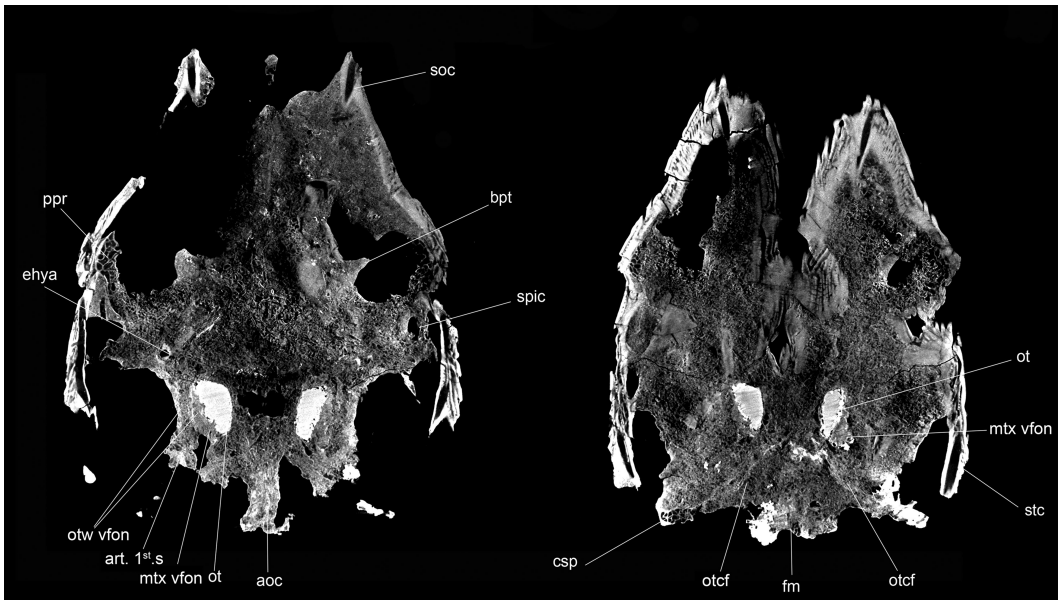

Figure 13 *Rhadinichthys bearsdeni* comb. nov. (formerly *Woodichthys*), axial view tomographic slices revealing internal anatomy of the braincase. Abbreviations: aoc = aortic canal; art. 1st.s = articulation for suprapharyngobranchial of first gill arch; bpt = basipterygoid process; csp = craniospinal process; ehya = canal or foramen for the efferent hyoid artery; fm = foramen magnum; mtx vfon = matrix infill of vestibular fontanelle; ot = otolith; otcf = oticooccipital fissure; otw vfon = otic wall and vestibular fontanelle; ppr = postorbital process; soc = supraorbital canal; spic = spiracular canal; stc = supratemporal canal.

The general proportions and distribution of features in ventral view are comparable to that of *Phoebeannaia* (Fig. 12d; Caron *et al*. 2023). The most obvious differences are the broad otic region and wide occipital plate in *R. bearsdeni* comb. nov., as well as the absence of any significant posteriorly projecting central unit of the occiput. In *R. bearsdeni* the aortic canal, notochordal cotylus, and foramen magnum are anteroposteriorly short.

Proceeding from anterior to posterior, with the parasphenoid removed virtually, the ventral surface of the basisphenoid is shown to have a well-marked midline groove passing posteriorly to the hypophyseal foramen, just as in *Phoebeannaia*. Likewise, in both taxa the hypophyseal foramen is level with the rear of the basipterygoid processes. There is no laterally prominent postorbital process in *R. bearsdeni* comb. nov. Instead, the process appears to have projected ventrally and now protrudes through the ascending rim of the broad lateral commissure (on the right side of the specimen). µCT data has revealed the presence of spiracular canal and a foramen for the efferent hyoid artery piercing the posterior rim of the spiracular groove (Figs 12b, 13). The facet for the hyomandibula is situated on the rear of the lateral commissure, dorsal to the posterior exit of the jugular canal.

The roof of the subtemporal fossa is broad; notably broader posteriorly than in *Phoebeannaia* (compare Fig. 12a and d). The ventral extremity of the otic wall is marked most clearly by the prominence of the articular process for the first suprapharyngobranchial. This process projects from the dorsal rim of the vestibular fontanelle, as in *Phoebeannaia* and *Kansasiella*, but is barely evident in Devonian taxa: *Mimipiscis* and *Raynerius* (Gardiner 1984; Giles *et al*. 2015). The full extent of the vestibular fontanelle is not immediately clear because a large otolith has punched through the anterior portion of this region on both sides of the braincase. Virtual removal of the otoliths provides an improved picture (Fig. 12b). The location of the otic-occipital fissure and the incomplete outline of the vestibular fontanelle is discernible in slices from the µCT stack (Fig. 13), confirming the previous radiograph-based interpretation (Coates 1998). The occipital plate is broad and terminates laterally with well-formed left- and right-side craniospinal processes. The midline structures of the plate are flanked by shallow concavities.

Unlike other Carboniferous neurocranial examples, such as *Lawrenciella, Kansasiella, Kentuckia*, and *Phoebeannaia* (summarised in Caron *et al*. 2023), the ventral otic fissure (Fig. 12a, b) cuts straight across the ventral surface; there is no convexity to the rear margin of the prechordal portion of the basicranium. Within the otic regions, the semicircular canals are not preserved in either specimen, but the otoliths are remarkably intact (see otolith section for details). Just anterior to the otolith is a small projection that might be the articular surface for the first infrapharyngobranchial (Fig. 12a, b). The articulation for the first suprapharyngobranchial (Fig. 11a, b) is more clearly resolved, and located posterior and lateral to the otolith.

The aortic canal (aoc, Fig. 12a, b) barely extends beyond the posterior boundary of the braincase. µCT scans reveal no hint of an internal septum, but it appears likely that the dorsal aorta divided into the lateral aortae within the canal, similar to *Raynerius, Phoebeannaia,* and *Coccocephalus* (Poplin & Véran 1996; Figueroa *et al*. 2023). A large foramen for the efferent branchial arteries (ebra, Fig. 12a, b) pierces the aortic canal near its caudal end, matching a similar opening in *Phoebeannaia*. The foramen magnum (fm, Fig. 12c) is identifiable as a shallow indentation close to the dorsal surface. Inspections of µCT scans show that the notochordal canal was obliterated as a result of postmortem compression; the anterior reach of the notochord is unknown.

3.3.3. Otoliths. The previous description reported a single pair of large, pear-shaped otoliths in NMS G.1984.42.15.c. Here, µCT scanning of the specimen has revealed a much smaller additional otolith, resting by the anterodorsal apex of the larger one (Fig 14a–c, e, f). GLAHM 163425a yielded left and right large otoliths of the same shape, also including a single

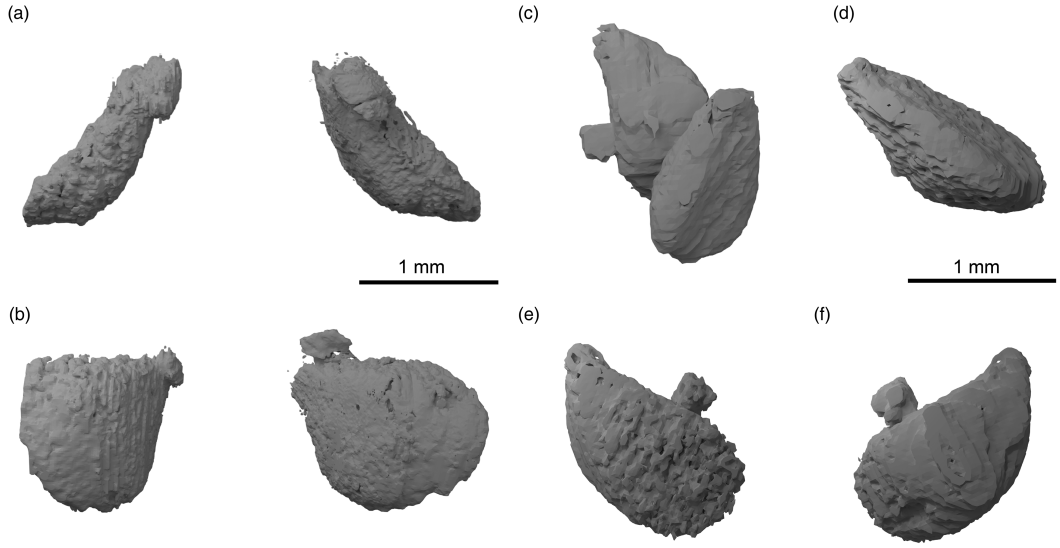

Figure 14 *Rhadinichthys bearsdeni* comb. nov. (formerly *Woodichthys*), three-dimensional renderings of the otoliths. (a) Left and right otoliths preserved in NMS G.1984.42.15.c, front view. (b) NMS G.1984.42.15.c left and right otoliths, ventral view. (c) GLAHM 163425a otoliths, left tipping out of the page. (d) GLAHM 163425a, left otolith. (e) GLAHM 163425a, right otoliths, lateral view. (f) GLAHM 163425a, right otoliths, mesial view.

accessory small otolith on the right side (Fig 14c–f). These small otoliths are ellipsoidal in shape, with a major axis spanning no more than 25 % of the maximum length of the larger otoliths. In anterior view, the left and right large otoliths of NMS G.1984.42.15.c lean away from each other at a gentle slope (Fig. 14a). From comparison with polypterid examples, Coates (1998) interpreted the large otolith as the asteriscus from the lagenar portion of the vestibular chamber. A central sulcus is clearly visible on the notional asteriscus from the left side. The smaller otolith is likely to be a lapillus from the utricular chamber, but in the absence of labyrinth infilling, identification remains conjectural.

3.3.4. Hyoid arch. A well-preserved left hyomandibula and interhyal are exposed on the surface of GLAHM 163425a, both of which appear to be completely ossified (Figs 4, 15, 16). The right hyomandibula is revealed by µCT data but provides no more than corroboration of details exposed on the left side of the hyoid arch. The dorsal and ventral limbs of the hyomandibula are of approximately equal length. The dorsal limb expands proximally, while the ventral limb is uniformly narrow with no hint of the distal expansion present in outgroups and seemingly primitive examples (Giles *et al.* 2015, 2023). The shape (an asymmetric boomerang) resembles that of *Pteronisculus* as depicted by Véran (1988). The angle between dorsal and ventral limbs is of around 150 degrees. There is no distinct or peg-like opercular process, but rather an elongate crest that probably articulated with the anteromedial rim of the opercular. This is much clearer in the photograph (Fig. 16a) than in the scan rendering (Fig. 15). The hyomandibula is imperforate, and the dermohyal is fused to the dorsal limb, represented by a few subparallel ornament ridges.

The interhyal is short and subcylindrical (Fig. 16b). This interhyal is the same as the hyoid arch bone identified as the symplectic by Véran (1988) for *Boreosomus*, *Pygopterus*, *Pteronisculus*, and others. The proximal articular facet matches the distal width of the hyomandibula. The distal facet is broader and oriented anteroventrally. The brief shaft of the interhyal is waisted. Whether the anterodistal facet articulated with the mandible and/or a proximal ceratohyal or other intermediate hyoid bone is unknown.

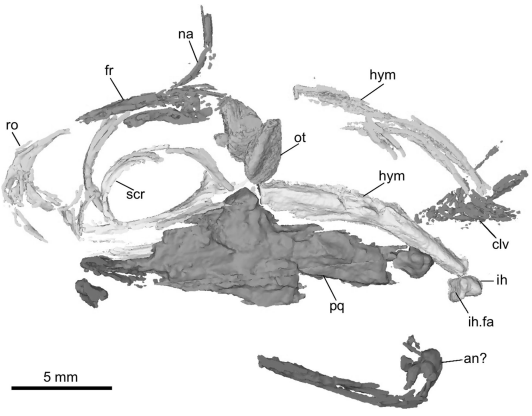

Figure 15 *Rhadinichthys bearsdeni* comb. nov. (formerly *Woodichthys*), µCT 3D reconstruction for GLAHM 163425a and b. Abbreviations: an = angular; clv = clavicle; fr = frontal; hym = hyomandibula; ih = interhyal; ih.fa = articular facet of the interhyal; na = nasal; ot = otolith; pq = palatoquadrate; ro = rostral; scl = supracleithrum; scr = sclerotic ring.

4. Discussion and conclusion

Rhadinichthys persists as one of the most long-standing and geographically widespread genera of Palaeozoic ray-finned fishes. However, attempts to place *Rhadinichthys* within a well-supported phylogeny or locate it within a broader palaeobiological context have been handicapped by a succession of ill-defined diagnoses. These various definitions have allowed the accumulation of around 27 species (Schultze *et al.* 2021) whose characteristics sometimes even contradict bounds of the enclosing generic diagnosis (Henderson *et al.* 2023). The solution offered here is to reduce genus membership to a definable core assembled from a data set consisting of the original type specimens supplemented with a more completely preserved neotype.

Regrettably, this action leads to the loss of '*Woodichthys*' (Coates 1998) as a distinct genus: a taxon named in honour of

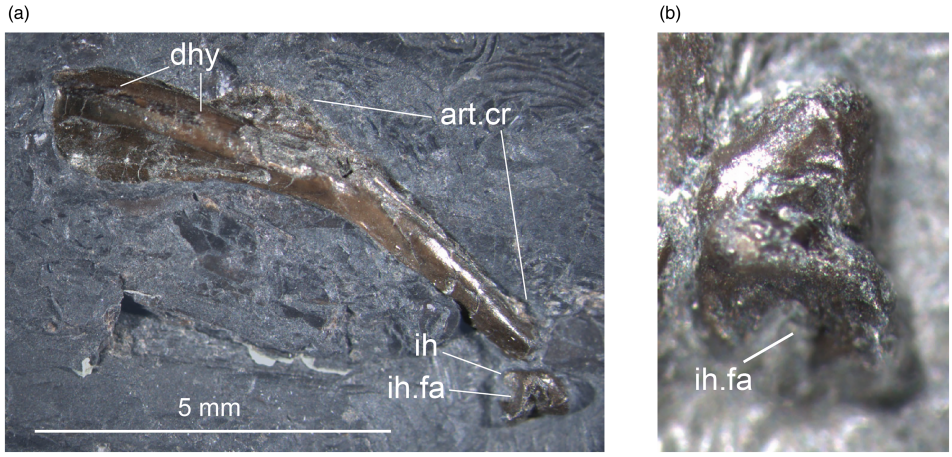

Figure 16 *Rhadinichthys bearsdeni* comb. nov. (formerly *Woodichthys*), photographs of the left hyoid arch from GLAHM 163425a. (a) The hyomandibula and the interhyal. (b) Close-up of the interhyal, articular facet facing left. Abbreviations: art.cr = articular crest; dhy = dermohyal; ih = interhyal; ih.fa = articular facet of the interhyal.

the late Stan Wood, whose extraordinary career in Palaeozoic fossil discovery was founded on collecting precisely these fishes, alongside many others, from the Lower Carboniferous of the Scottish Midland Valley. *Woodichthys* (Coates 1998) was established as a discrete taxonomic entity because the author (MIC), in the course of that project, failed to recognise similarities other than general resemblances shared with the type material of *Rhadinichthys*. In the present study, re-examination of *Woodichthys* uncovered new derived features which, in turn, led to a thorough re-evaluation of dermal skeletal details in the type species of both genera. In particular, μCT re-examination of the *Woodichthys* skull table revealed sutures defining the true shape of the supratemporal. This could be described as 'cleaver-shaped' or shaped like the state of Oklahoma (USA), with a distinct 'handle' that wraps around the flank of the frontal. Importantly, this unusual supratemporal shape is also evident in *Rhadinichthys ornatissimus*. A further synapomorphy uniting *Woodichthys* and *Rhadinichthys* is evident in the ornament and shape of the rostral bone, the characteristic details of which are discussed below. Further to these features, additional shared specialisations, perhaps with more homoplastic distributions, include the elongate slat-like proximal lepidotrichia of the pectoral fins, the ornamentation of the preoperculum (divided into dorsal and ventral zones), the irregular distribution of the pores in the lateral line scales, and the numbers of fulcral scales preceding midline fins.

Faced with these shared derived features, possible taxonomic actions might be to remove *ornatissimus* from the genus *Rhadinichthys* and reassign it to *Woodichthys*, or, vice versa, to subsume *W. bearsdeni* within *Rhadinichthys*. On the grounds of systematic stability, because *ornatissimus* is the type species of *Rhadinichthys*, we propose the second taxonomic act: to subsume the genus *Woodichthys* within the redefined *Rhadinichthys*. A third alternative, to maintain both genera, would be the least useful (taxonomic inaction), with the two taxa separated by minor differences of dermal ornament, fin position and scale count. To all intents and purposes, *Woodichthys bearsdeni* and *Rhadinichthys sensu stricto* would then be treated as the same operational taxonomic unit. In effect, this would be a taxonomic act deferred, given that a principal aim of phylogenetic systematics is the discovery of natural supraspecific groups (e.g., Wiley 1981; Smith 1994).

The assembly of these revised descriptions draws attention to a short list of features that deserve further comment. The first is the ornamentation of the rostral bone. In general, the value of dermal ornament as a signal of relatedness, especially among early actinopterygians, is limited. Hence, the pattern of sinuous ridges on all large dermal bones of *Rhadinichthys ornatissimus* and *R. bearsdeni* comb. nov., bears a general resemblance to the ornament of *Cosmoptychius* (Traquair 1877b, pl. 3, fig. 3), *Mesonichthys* (Traquair 1901, pl. 17, fig. 7; British Geological Survey Collections specimen GSL 1311, pers. obs., MIC), and even *Mimipiscis* (Gardiner 1984, fig. 79), among many other examples. These instances have yet to be linked to any other characteristics that might define a discrete clade among the abundance of early ray-finned fishes. Rather, these repeated occurrences probably reflect functional and/or developmental biases. However, we argue that the rostral bone ornament and shape in *R. ornatissimus* and *R. bearsdeni* comb. nov. is a valid genus-level diagnostic feature (Fig. 8a, b). In particular, we draw attention to the marked switch in ornament type between cap and plate, the straight posterior rim, and the naked (ornament-free) zone anterior to the anterior nostril notch. Once more, comparison with *Mimipiscis* is useful: Gardiner (1984, fig. 79) depicts a rostral with ridge ornament covering posterior plate and continuous with snout cap regions. There is no clear margin at the nasal notch, and a convex posterior boundary protrudes between the frontals. A further instance of the utility of rostral ornament is demonstrated in *Trawdenia* (Coates & Tietjen 2018). In this example the bulbous rostral ornament unites three species extracted from the genus *Mesopoma* (incidentally including a former species of *Rhadinichthys*: '*R. planti*'). We suggest that, at genus level, rostral ornament can provide a more systematically useful badge than characteristics of the general dermal ornament.

The temporal bone series presents a second dermatocranial feature deserving brief discussion. *Rhadinichthys* as defined here has two canal-bearing bones, a long and posteriorly broad supratemporal and a short intertemporal, connected in series to the rear of the dermosphenotic. Two-bone temporal series are widespread among Devonian actinopterygians (e.g., Gardiner 1984) and probably represent a plesiomorphic condition relative to presence of a single bone, a dermopterotic, as found in many more recent taxa (Gardiner & Schaeffer 1989; Grande 2010). The different arrangements, complements, and terminologies applied to these temporal bones have been discussed at length elsewhere, with contrasting arguments presented in works such

as Pearson & Westoll (1979), Gardiner & Schaeffer (1989), and Schultze *et al*. (2021). The relevance to the present study is that many species currently attributed to *Rhadinichthys* (see Table 1) have a single temporal bone: a dermopterotic. Notably, these dermopterotic-bearing species include some of the classic (i.e., often depicted) members of *Rhadinichthys*, such as *R. canobiensis* and *R. fusiformis* from the Glencartholm fauna (Moy-Thomas & Bradly Dyne 1938). It now appears that these species, if described accurately, belong elsewhere (a point returned to later).

The neurocranium is arguably the most important addition to the *Rhadinichthys* data set. Although μCT scans have added only modestly to previously available information, the broader phylogenetic context has changed, and more materials are now available for comparative evaluation. The *Rhadinichthys* neurocranium appears very similar to those of *Phoebeannaia*, *Kansasiella* (Caron *et al*. 2023), and *Coccocephalus* (Figueroa *et al*. 2023). A modest distinction is evident in the width of the posterior portion of the otic region, the corresponding breadth of the occipital plate, and the minimal posterior projection of the occipital unit. In other respects, these crania are mostly alike with spiracular canals, aortic canals, similarly positioned cranial fissures, large vestibular fontanelles, locations of major foramina, and prominent basipterygoid processes. *Rhadinichthys* provides a minor variation on what appears to be a morphotype common to many fusiform Carboniferous actinopterygians. Resolving relationships among these taxa is proving difficult, and comparisons with the neurocrania of living non-neopterygians (i.e., polypterids and chondrosteans) emphasises the morphological distance between extant so-called primitive actinopterygians and Palaeozoic examples (cf. discussion in Caron *et al*. 2023).

As for the otoliths in *R. bearsdeni*, existing reviews and discussions (Coates 1998; Friedman & Giles 2016; Schultze *et al*. 2021) note that while extant actinopterygians have three (utricular, saccular, and lagenar otoliths), the record of Palaeozoic examples is extremely uneven. Most discussion revolves around whether one or two otoliths were present in the *pars inferior*. The small otolith newly discovered in *R. bearsdeni* could either be the utricular otolith from the *pars superior* (as identified in the description) or the second *pars inferior* otolith. Of uncertain significance, the most similarly shaped large otoliths in extant fishes are the lagenar otoliths of polypterids (Coates 1998). Aside from *R. bearsdeni*, *Coccocephalus wildi* is the only other early Carboniferous taxa with three-dimensional μCT scanned otoliths, but this reveals only a single large pear-shaped otolith present in each *pars inferior* chamber (Figueroa *et al*. 2023; see also the depiction of a single otolith in latest Carboniferous–earliest Permian actinopterygian in Figueroa *et al*. 2024).

The present redefinition of *Rhadinichthys* prompts further evaluation of phylogenetic placement, especially in the context of the broad systematic frameworks provided by Schultze *et al*. (2021), and Giles *et al*. (2023). Furthermore, the most recent depiction of *R. ornatissimus* (Gardiner & Schaeffer 1989, fig. 16b) is quite unlike the material presented here, with dermopterotic, suborbitals, and a different dentition. This previous version, as noted in the introduction, suggests affinities with genera such as the Upper Carboniferous genus *Amblypterus*. However, if '*Woodichthys*'/*Rhadinichthys* is employed as a guide for placement in previous phylogenetic hypotheses, then there is a general trend through successive analyses to move the genus out of the actinopterygian crown. Coates (1999) placed '*Woodichthys*' on the actinopteran stem, but Cloutier & Arratia (2004) resolved '*Woodichthys*' as a stem actinopterygian, a result that has persisted throughout a series of subsequent phylogenies. '*Woodichthys*' is often placed in these as sister-group to all other Carboniferous taxa (e.g., Choo *et al*. 2019; Giles *et al*. 2023). In contrast, Caron *et al*. (2023), using a data set based solely on endocranial characters, generated trees that hint at a different solution. If *Phoebeannaia* is used as a proxy for *Rhadinichthys* (given the neurocranial similarity) then the genus probably occupies a more nested position among the Carboniferous actinopterygian radiation. However, consistent with the preceding discussion of the neurocranium, the wider phylogenetic significance of this clustering has yet to be determined. At a more parochial level of relationships, *Rhadinichthys* is the exemplar for a collection of genera grouped as rhadinichthyids (Lund & Poplin 1997; Schultze *et al*. 2021). Rhadinichthyid members also include the South African genus *Mentzichthys* and Bear Gulch taxa such as *Wendyichthys* and *Cyranorhis*. Relative to other Carboniferous actinopterygians, none of these appears especially close to the present definition of *Rhadinichthys*, particularly in the composition of the dermal skull and the elaborate patterns of regionalised squamation. It is unlikely that rhadinichthyids in the currently published sense will survive further examination.

To conclude this overview, few of the 27 or so *Rhadinichthys* species are likely to remain in the genus. Table 1 provides a summary, in which all current members (as listed in Schultze *et al*. 2021) are compared to the new genus diagnosis. Out of the total of 27 species (including *R. ornatissimus* and *R. bearsdeni*), 14 lack sufficient data to determine their status as *Rhadinichthys*. This is hardly surprising given the incomplete condition of many fossil actinopterygians, and it seems that '*Rhadinichthys*' species from the extremities of the temporal range (Devonian and Permian examples) are among the worst preserved and least characterised. Ten species are excluded because they clearly contradict the genus diagnosis. Several bear a dermopterotic rather than intertemporal and supratemporal bones. Consequently, *R. canobiensis*, perhaps the most widely cited and depicted of *Rhadinichthys* species (e.g., Moy-Thomas & Miles 1971) belongs elsewhere. This leaves a mere four species: *R. ornatissimus*, *R. bearsdeni*, *R. ferox*, and *R. laevis*, all of which are from the uppermost part of the Middle Mississippian and the earliest Late Mississippian of Scotland.

Rhadinichthys viewed in this light assumes a more morphologically, spatially, and temporally confined identity. *Rhadinichthys laevis* from Tarras Water Foot, Eskdale, is a probable outlier of the classic Glencartholm fish fauna (Dineley & Metcalf 1999), characterised as inhabiting a nearshore marine environment. *Rhadinichthys ornatissimus* and *R. ferox* originate from the Oil Shales of the Scottish Midland Valley, deposited on the floor of a lagoonal environment, Lake Cadell (Loftus & Greensmith 1988), up to 50 km wide (Dineley & Metcalf 1999) and approximately coeval with Glencartholm. *Rhadinichthys bearsdeni* is the youngest of the set, coming from the marine deltaic environments of the Manse Burn Formation. The time span of the entire genus now ranges from approximately 335 Ma to 328 Ma, a modest seven million years, (much reduced relative to former estimates) with species ranging from marine into non-marine habitats. The quantity and geographic spread of *R. ornatissimus* material suggests that it thrived in the Oil Shale lagoon, with individuals present in collections from many if not all of the major Victorian oil shale works: Straiton, Broxburn, and elsewhere (Clarkson & Upton 2006). Other actinopterygian genera of the biota (summarised from the Wardie ichthyofaunal list of Dineley & Metcalf 1999) include *Eurynotus* (= *Notacmon*, Schultze *et al*. 2021), *Nematoptychius*, *Cosmoptychius*, *Gonatodus*, *Wardichthys*, and *Elonichthys*. Sarcopterygians include *Rhizodus*, *Megalichthys*, and unidentified lungfish, while the sharks include *Acanthodes*, *Diplodoselache*, *Tristychius*, and *Sphenacanthus*. Many of these fishes approach or exceed a metre or more in length, in contrast

Table 1 Preliminary assessment of existing *Rhadinichthys* species in light of the new generic diagnosis, with comments on their gross morphology. Observations (except for *R. ornatissimus* and *bearsdeni* comb. nov.) are based on published specimen photos and illustrations.

Species	Locality and age	*Rhadinichthys*?	References
R. ornatissimus Traquair, 1877	Flex Coal, Carboniferous Limestone, Limestone Coal Formation, Lothian, Scotland, Serpukhovian, Upper Mississippian, Carboniferous; Ballagan Formation, Midlothian and Fifeshire, Scotland; Abbeyhill Shales Beds, Craighleith Quarry Sandstones, and Wardie Shales Member, Gullane Formation, Lothian, Scotland, Viséan, Middle Mississippian, Carboniferous	**Type**	Traquair (1911, pp. 127–130, pl. XXVIII), NMS G.1878.18.7, NMS G.1896.147.1, NMS G.1891.24.11, NMS G.1859.33.66, NMS G.1889.115.3, MCZ 10620
R. alberti Jackson, 1851	Albert Shale Formation, New Brunswick, Canada, Tournaisian, Lower Mississippian, Carboniferous	**Not *Rhadinichthys*** • Large fulcra scales lining the entire dorsal side of the fish • No lateral line scale piercings • Proliferation of small-scale rows at the base of the pelvic and anal fins	Mickle (2017, pp. 52–53)
R. argentinicus Tornquist, 1904	Estancia Carpinteria between San Juan and Mendoza, Argentina, Upper Carboniferous	**Insufficient data** • Pectoral lepidotrichia do not bifurcate	Schultze *et al.* (2021, p. 130)
R. bearsdeni comb. nov. Coates, 1998	Manse Burn Formation, Bearsden, Scotland, Pendleian (Namurian) E1 Zone, Mississippian, Carboniferous	**Yes**	Coates (1998) and μCT data from NMS G.1984.42.15.c and GLAHM 163425a and b
R. brevis Traquair, 1877	Wardie Shales Member, Gullane Formation, Lothian, Scotland, Viséan, Middle Mississippian, Carboniferous	**Insufficient data** • Similar body proportions and lower jaw ornaments to *Rhadinichthys*, no diagnostic detail reported	Traquair (1911, pp. 143–144, pl. XXXI; figs 7–10)
R. canobiensis Traquair, 1909a	Glencartholm Volcanic Member, Tyne Limestone Formation, Dumfriesshire, Scotland, Viséan, Middle Mississippian, Carboniferous	**Not *Rhadinichthys*** • Dermopterotic present • High snout apex • Path of supraorbital canal follows a straight course and exits the frontal anterolaterally, different from *R. beardeni*	Traquair (1911, pp. 133–137, pl. XXX), Moy-Thomas & Bradley Dyne (1938, figs 14–16)
R. carinatus Traquair, 1877	Extensive distribution in the Lower Carboniferous rocks of the Great Central Valley of Scotland	**Not *Rhadinichthys*** • Dermopterotic present • Different body proportions from *Rhadinichthys*: small head relative to body; short tail; small paired fins and large median fins • Deeper body shape than *Rhadinichthys*	Traquair (1911, pp. 130–133, pl. XXIX, figs 1–6), Gardiner & Schaeffer (1989, fig. 1e)
R. devonicus Clark, n.d.	Portage Formation/Kettle Point Formation, Lambton County, Ontario, Canada; Wietrznia Beds, Holy Cross Mountains, Poland; Bahram Formation, Tabas region, Eastern Iran Frasnian, Lower Devonian Genesee Formation, Appalachian basin, New York State, USA, Frasnian to Famennian, Lower Devonian;	**Insufficient data** • Known from scales and isolated remains	Rayner (1952, p. 55)
R. ferox Traquair, 1877	Ironstone nodules from Wardie, near Edinburgh, West Lothian Oil Shale Formation, Scotland, Viséan, Middle Mississippian, Carboniferous	**Candidate** • Long proximal unsegmented lepidotrichia – synapomorphy of *Rhadinichthys*	Traquair (1911, pp. 153–154, pl. XXXIV, figs 1, 2)
R. flexuosus Yankevich, 1998	East European Platform, Russia, Artinskian, Lower Permian	**Insufficient data** • Represented by isolated scales	Schultze *et al.* (2021, p. 132)
R. formosus Traquair, 1904	Cheese Bay Shrimp Bed, Gullane Formation, East Lothian, Scotland, Viséan, Middle Mississippian, Carboniferous	**Insufficient data** • Shattered cranium and incomplete post-cranium, no distinguishing synapomorphy with *Rhadinichthys*	Traquair (1911, pl. XXXIV, fig. 3)
R. glabrolepis Elliot, 2016	Upper Slatyband Ironstone Shale, Scottish Lower Coal Measures Formation, Greenrigg, Midland Valley of Scotland, Westphalian A (Bashkirian), Pennsylvanian, Carboniferous	**Not *Rhadinichthys*** • Dermopterotic present • Length:width proportion of the maxilla close to 1, suggesting that this fish does not have upright jaw suspension; *Rhadinichthys* has a longer posterior portion of the maxilla and a far more steeply inclined (vertical) gape	Elliot (2016)

(*Continued*)

Table 1 Continued.

Species	Locality and age	*Rhadinichthys?*	References
R. grossarti Traquair, 1878	Scottish Lower Coal Measures Formation, Lanarkshire and Midland Valley, Scotland, Westphalian A, Upper Carboniferous; France and Belgium, Westphalian D, Lower Pennsylvanian, Carboniferous	**Not *Rhadinichthys*** • Dermopterotic present • Tubercular ornamentation on skull roof unknown in *Rhadinichthys* • Parietal diminutive and without pit lines • Parasphenoid lozenge shaped, ascending process slender not broad • No basipterygoid process • Gross morphology suggests it to be a more derived fish than *Rhadinichthys*, similar to *Trawdenia*	Traquair (1911, pp. 150–151, pl. XXXIII, figs 7–8), Elliot (2016), Derycke *et al.* (1995)
R. hancocki Atthey, 1875	Pennine Middle Coal Measures Formation, Newsham, Northumberland; 'Better Bed' Coal, Low Moor, Yorkshire, England, Bashkirian, Lower Pennsylvanian, Carboniferous	**Insufficient data** • Preserved materials include the trunk and a splintered cranium, no distinguishing synapomorphy	Traquair (1911, pp. 147–149, pl. XXXIII, figs 1, 2)
R. hibernicus Traquair, 1911	Coolbaun Formation, Jarrow Colliery, Kilkenny County, Leinster, Ireland, Westphalian, Lower Pennsylvanian, Carboniferous	**Insufficient data** • Fusiform body • Dorsal fin parallel to the level of anal fin • Cranium partially eroded and preserved no distinguishing synapomorphy	Traquair (1911, pp. 144–146, pl. XXXII, figs 1, 2)
R. laevis Traquair, 1911	Ballagan Formation, Tarras Water Foot, Eskdale, Scotland, Viséan, Middle Mississippian, Carboniferous	**Candidate** • The following features are similar to *Rhadinichthys*: maxilla and jaw proportions; prearticular and pterygoid shapes, known from impressions on the palatal side; fulcra scale arrangement; body shape – humped back; pectoral fin rays unarticulated until near their termination; scales are smooth with just a few pores, like *R. bearsdeni*	Traquair (1911, pp. 149–150, pl. XXXIII, figs 3–6)
R. lerichei Pruvost, 1919a	Belgium and Northern France, Moscovian (Westphalian D), Upper Carboniferous	**Insufficient data** • Represented by isolated scales	Schultze *et al.* (2021, p. 132), Derycke *et al.* (1995)
R. macconochii Traquair, 1881	Glencartholm, Dumfries and Galloway, Scotland, Viséan, Middle Mississippian, Carboniferous	**Insufficient data** • Possibly not *Rhadinichthys* – its diagnosis states that the arrangement of cranial bones is as in *R. canobiensis*	Traquair (1911; pl. XXIX, figs 7–11)
R. macrodon Traquair, 1877	Knowles Ironstone Shale, Longton, Staffordshire, 'Better Bed' Coal, Low Moor, Yorkshire, England, Moscovian, Middle Pennsylvanian, Carboniferous	**Not *Rhadinichthys*** • Large teeth – in contrast, *Rhadinichthys* has uniform small teeth with minute marginal ones	Traquair (1911, pp. 146–147, pl. XXXII, figs 3–5)
R. monensis Egerton, 1850	Pennine Lower Coal Measures Formation, Foxfield Colliery, Staffordshire, England; Upper Drumgray, Scottish Lower Coal Measures Formation, Ardenrigg, Midland Valley, Scotland, Scottish Lower Coal Measures Formation, North Lanarkshire, Scotland, Bashkirian, Lower Pennsylvanian, Carboniferous; France and Belgium, Westphalian A to B, Pennsylvanian, Carboniferous	**Not *Rhadinichthys*** • Dermopterotic present • Parasphenoid with no basipterygoid process and long, extending ascending process	Traquair (1911, pp. 137–139, pl. XXXI, figs 3–6), Elliot (2016), Derycke *et al.* (1995)
R? ornatocephalum Elliot, 2016	Found in all localities where Drumgray shales are exposed, Westphalian A (Bashkirian), Lower Pennsylvanian, Carboniferous	**Not *Rhadinichthys*** • Dermopterotic present • Circumvoluted dermal ornaments	Elliot (2016)
R? plumosum Elliot, 2016	Carbonaceous shale at Wester Bracco coal waste tip in North Lanarkshire, Scotland, Westphalian A, Lower Pennsylvanian, Carboniferous	**Not *Rhadinichthys*** • Shape of maxilla unlike *Rhadinichthys*; anterior to posterior maxilla proportion suggests that this fish does not have a long gape	Elliot (2016)
R. renieri Pruvost, 1919a	Chokier Formation, Belgium, Serpukhovian to Bashkirian, Carboniferous	**Insufficient data** • Represented by isolated scales	Schultze *et al.* (2021, p. 132), Derycke *et al.* (1995)
R? rioniger Beltan, 1977	San Gregorio Formation, Rio Negro, Uruguay, Sakmarian + Asselian, Lower Permian	**Insufficient data** • Possessing a single dermosphenotic and possibly two paired extrascapulae; other conditions uncertain	Schultze *et al.* (2021, p. 132)
R. silvensis Yankevich, 1998	Ufimian (Kungurian) deposits of the Pechora Coal Basin, Lower Permian of the Northern Urals, Russia	**Insufficient data** • Known from body fragments	Schultze *et al.* (2021, p. 132)

(*Continued*)

Table 1 Continued.

Species	Locality and age	*Rhadinichthys?*	References
R. tuberculatus Traquair, 1881	Glencartholm, Dumfries and Galloway, Scotland, Viséan, Middle Mississippian, Carboniferous; Southern Belarus, East European platform, Upper Famennian, Devonian	**Insufficient data** • Anterior half of the illustrated specimen shattered, no distinguishing synapomorphy preserved	Traquair (1911; pl. XXXV, fig. 1)
R. wardi Traquair, 1877	Deep Mine Ironstone Shale, Pennine Middle Coal Measures Formation, Longton, Staffordshire, England, Westphalian A to C, Pennsylvanian, Carboniferous; Scottish Lower Coal Measures Formation, North Lanarkshire and Midland Valley, Scotland, Westphalian A, Pennsylvanian, Carboniferous	**Insufficient data** • Illustrated specimen has undergone substantial erosion, anatomical details indistinguishable except for a notable big gape	Traquair (1911, pp. 142–143, pl. XXXI, figs 1, 2)

with the ten centimetres or more of *Rhadinichthys*. Therefore, as one of the smallest members of the lagoonal fish biota, and alongside the abundant shrimps, it seems likely that this study provides a more informed picture of one of the lower components of the Scottish Late Mississippian aquatic food chain. *Rhadinichthys* might be diminutive in these respects but now, data enriched, it represents a potentially useful addition to aid resolution of the Devonian–Carboniferous actinopterygian evolutionary radiation (Caron *et al*. 2023; Giles *et al*. 2023).

Finally, the current study presents an exercise in the treatment of wastebasket taxa. In many instances such groups embody a history in which an initially monophyletic (and often monospecific) genus accretes taxa until it balloons into para- or polyphyletic status, i.e., transforms from diagnosable clade to grade or, eventually, a nominal cluster with boundaries set by arbitrary convention (Smith 1994). The original specimens, usually the type material, often lack the detail of subsequent discoveries, and these, in turn, tend to be extracted to form a hierarchy of more precisely defined groups. Meanwhile, the characteristics of the original specimens, first identified as apomorphies, are re-evaluated as plesiomorphies of a larger and more diverse entity. In this way, wastebasket taxa may be eliminated via successive taxonomic extractions. Among Palaeozoic vertebrates, *Labyrinthodon* (see Desmond 1982 for historical context) and the Labyrinthodontia (for evolving views see Romer 1966; Carroll 1988; Clack 2002) present a good example. Others, however, survive because a kernel of systematic value persists and is built upon via new discoveries and redefinition. *Rhadinichthys* represents one such, but it also exemplifies a smaller version of the problem with palaeoniscids (see Palaeoniscimorpha in Schultze *et al*. 2021; for a history of the term in various forms see Gardiner & Schaeffer 1989). The major challenges are (1) to discover the appropriate stem groups to which members of this vast grade belong (Jefferies 1986) and (2) to determine whether a diagnosable, monophyletic rump group exists to which this name might be applied. For the present, this remains unresolved (Giles *et al*. 2017, 2023; Caron *et al*. 2023).

5. Acknowledgements

We thank the editors for the invitation to contribute to this volume honouring the work of Dr Tim Smithson. Patrick Gavin is thanked for the discovery and donation of the new specimen of *Rhadinichthys bearsdeni* to the collections of the Hunterian Museum, University of Glasgow. Neil Clark is thanked for providing access to the Hunterian Museum, University of Glasgow collections. Nick Fraser and Stig Walsh are thanked for providing access to the collections of the National Museums of Scotland; likewise, Stephanie Pearce for access to the collections of the Comparative Museum of Zoology, Harvard University, USA. Mark Webster, University of Chicago, provided valuable advice to the lead author during the initial phase of this project. April Neander is thanked for assistance with use of the PaleoCT facility, University of Chicago. We are most grateful to two anonymous reviewers for their insights, suggestions, and especially for assistance with updates on the geological settings. This study was partially supported by NSF EAR 2218892 (MIC).

6. Competing interests

The authors declare none.

7. References

Agassiz, L. 1835. *Recherches sur les poissons fossiles: une introduction à l'étude de ces animaux*. Tome 2. Neuchatel: Imprimerie de Petitpierre et Prince.

Aretz, M., Herbig, H.-G., Wang, X., Gradstein, F., Agterberg, F. & Ogg, J. 2020. The Carboniferous period. In *Geologic Time Scale 2020*, 811–74. Amsterdam: Elsevier.

Caron, A., Venkataraman, V., Tietjen, K. & Coates, M. 2023. A fish for Phoebe: a new actinopterygian from the upper carboniferous coal measures of Saddleworth, Greater Manchester, UK, and a revision of *Kansasiella eatoni*. *Zoological Journal of the Linnean Society* **198**, 957–81.

Carroll, R. L. 1988. *Vertebrate Paleontology and Evolution*. New York: W. H. Freeman and Company.

Choo, B., Lu, J., Giles, S., Trinajstic, K. & Long, J. A. 2019. A new actinopterygian from the Late Devonian Gogo Formation, Western Australia. *Papers in Palaeontology* **5**, 343–63.

Clack, J. A. 2002. *Gaining Ground. The Origin and Evolution of Tetrapods*. Bloomington: Indiana University Press.

Clark, N. D. L. 1989. A study of a Namurian crustacean-bearing shale from the western Midland Valley of Scotland. PhD Thesis, University of Glasgow, UK.

Clarkson, E. & Upton, B. 2006. *Edinburgh Rock, the Geology of Lothian*. Edinburgh: Dunedin Academic Press.

Cloutier, R. & Arratia, G. 2004. Early diversification of actinopterygians. In Arratia, G., Wilson, M. V. H. & Cloutier, R. (eds) *Recent Advances in the Origin and Early Radiation of Vertebrates*, 217–70. München: Verlag Dr Friedrich Pfeil.

Coates, M. I. 1988. A new fauna of Namurian (Upper Carboniferous) fish from Bearsden, Glasgow. Unpublished PhD Thesis, University of Newcastle Upon Tyne.

Coates, M. I. 1998. Actinopterygians from the Namurian of Bearsden, Scotland, with comments on early actinopterygian neurocrania. *Zoological Journal of the Linnean Society* **122**, 27–59.

Coates, M. I. 1999. Endocranial preservation of a Carboniferous actinopterygian from Lancashire, UK, and the interrelationships of primitive actinopterygians. *Philosophical Transactions of the Royal Society of London. Series B: Biological Sciences* **354**, 435–62.

Coates, M. I. & Tietjen, K. 2018. 'This strange little palaeoniscid': a new early actinopterygian genus, and commentary on pectoral fin

conditions and function. *Earth and Environmental Science Transactions of the Royal Society of Edinburgh* **109**, 15–31.
Community, BO 2018. *Blender – a 3D Modelling and Rendering Package*. Amsterdam: Stichting Blender Foundation.
Derycke, C., Cloutier, R. & Candilier, A. M. 1995. Palaeozoic vertebrates of northern France and Belgium: part II. Chondrichthyes; Acanthodii; Actinopterygii (uppermost Silurian to Carboniferous). *Geobios* **28**, 343–50.
Desmond, A. 1982. *Archetypes and Ancestors. Palaeontology in Victorian London 1850–1875*. London: Blond & Briggs.
Dineley, D. L. & Metcalf, S. J. 1999. *Fossil Fishes of Great Britain*, **16.** Peterborough: Joint Nature Conservation Committee.
Elliott, F. M. 2016. An early actinopterygian ichthyofauna from the Scottish Lower Coal Measures Formation: Westphalian A (Bashkirian). *Earth and Environmental Science Transactions of the Royal Society of Edinburgh* **107**, 351–94.
Figueroa, R. T., Goodvin, D., Kolmann, M. A., Coates, M. I., Caron, A. M., Friedman, M. & Giles, S. 2023. Exceptional fossil preservation and evolution of the ray-finned fish brain. *Nature* **614**, 486–91.
Figueroa, R. T., Weinschütz, L. C., Giles, S. & Friedman, M. 2024. Soft-tissue fossilization illuminates the stepwise evolution of the ray-finned fish brain. *Current Biology* **34**, 2831–40e2.
Friedman, M. & Giles, S. 2016. Actinopterygians: the ray-finned fishes – an explosion of diversity. In Clack, J. A., Fay, R. R. & Popper, A. N. (eds) *Evolution of the Vertebrate Ear: Evidence from the Fossil Record*, 17–49. Cham, Switzerland: Springer Handbook of Auditory Research **59**.
Friedman, M., Pierce, S. E., Coates, M. & Giles, S. 2018. Feeding structures in the ray-finned fish *Eurynotus crenatus* (Actinopterygii: Eurynotiformes): implications for trophic diversification among Carboniferous actinopterygians. *Earth and Environmental Science Transactions of the Royal Society of Edinburgh* **109**, 33–47.
Gardiner, B. G. 1984. The relationships of the palaeoniscid fishes, a review based on specimens of *Mimia* and *Moythomasia* from the Upper Devonian of Western Australia. *Bulletin of the British Museum (Natural History) Geology* **37**, 173–28.
Gardiner, B. G. & Schaeffer, B. 1989. Interrelationships of lower actinopterygian fishes. *Zoological Journal of the Linnean Society* **97**, 135–87.
Giles, S., Darras, L., Clément, G., Blieck, A. & Friedman, M. 2015. An exceptionally preserved Late Devonian actinopterygian provides a new model for primitive cranial anatomy in ray-finned fishes. *Proceedings of the Royal Society B: Biological Sciences* **282**, 20151485.
Giles, S., Feilich, K., Warnock, R. C., Pierce, S. E. & Friedman, M. 2023. A Late Devonian actinopterygian suggests high lineage survivorship across the end-Devonian mass extinction. *Nature Ecology & Evolution* **7**, 10–19.
Giles, S., Xu, G. H., Near, T. J. & Friedman, M. 2017. Early members of 'living fossil' lineage imply later origin of modern ray-finned fishes. *Nature* **549**, 265–68.
Grande, L. 2010. An empirical synthetic pattern study of gars (Lepisosteiformes) and closely related species, based mostly on skeletal anatomy. The resurrection of Holostei. *Copeia* **10**(2A), 1–871.
Hamel, M. H. & Poplin, C. 2008. The braincase anatomy of *Lawrenciella schaefferi*, actinopterygian from the Upper Carboniferous of Kansas (USA). *Journal of Vertebrate Paleontology* **28**, 989–1006.
Henderson, S., Dunne, E. M., Fasey, S. A. & Giles, S. 2023. The early diversification of ray-finned fishes (Actinopterygii): hypotheses, challenges and future prospects. *Biological Reviews* **98**, 284–315.
Huxley, T. H. 1880. On the applications of the laws of evolution to the arrangement of the Vertebrata and more particularly of the Mammalia. *Proceedings of the Zoological Society of London* **43**, 649–62.
Jefferies, R. P. S. 1986. *The Ancestry of the Vertebrates*. London: British Museum (Natural History).
Loftus, G. W. F. & Greensmith, J. T. 1988. The lacustrine Burdiehouse Limestone Formation – a key to the deposition of the Dinantian Oil Shales of Scotland. *Geological Society, London, Special Publications* **40**, 219–34.
Lund, R. & Poplin, C. 1997. The rhadinichthyids (paleoniscoid actinopterygians) from the Bear Gulch limestone of Montana (USA, Lower Carboniferous). *Journal of Vertebrate Paleontology* **17**, 466–86.
Materialise NV 2016. Materialise Mimics – 3D medical image segmentation software. Belgium.
Mickle, K. E. 2017. The lower actinopterygian fauna from the Lower Carboniferous Albert shale formation of New Brunswick, Canada – a review of previously described taxa and a description of a new genus and species. *Fossil Record* **20**, 47–67.
Monaghan, A. A., Browne, M. A. & Barfod, D. N. 2014. An improved chronology for the Arthur's seat volcano and Carboniferous magmatism of the midland valley of Scotland. *Scottish Journal of Geology* **50**, 165–72.
Moy-Thomas, J. A. & Bradley Dyne, M. 1938. The actinopterygian fishes from the Lower Carboniferous of Glencartholm, Eskdale, Dumfriesshire. *Earth and Environmental Science Transactions of the Royal Society of Edinburgh* **59**, 437–80.
Moy-Thomas, J. A. & Miles, R. S. 1971. *Palaeozoic Fishes*, 2nd edn. London: Chapman and Hall.
Nielsen, E. 1942. Studies on Triassic fishes from East Greenland 1: *Glaucolepis* and *Boreosomus*. *Meddelelsor om Gronland* **138**, 1–403.
Pearson, D. M. & Westoll, T. S. 1979. The Devonian actinopterygian *Cheirolepis* Agassiz. *Earth and Environmental Science Transactions of the Royal Society of Edinburgh* **70**, 337–99.
Poplin, C. 1974. *Étude de quelques Paléonsicidae Pennsylvaniens du Kansas*. Paris: Centre National de la Recherche Scientifique.
Poplin, C. 1975. *Kansasiella* nomen novum replacement *Kansasia* Poplin, 1974 (Poissons: Palaeonisciformes). *Bulletin de la Société Géologique de France* **17**, 26.
Poplin, C. & Véran, M. 1996. A revision of the actinopterygian fish *Coccocephalus wildi* from the Upper Carboniferous of Lancashire. *Special Papers in Palaeontology* **52**, 7–29.
Pradel, A., Maisey, J. G., Mapes, R. H. & Kruta, I. 2016. First evidence of an intercalar bone in the braincase of 'palaeonisciform' actinopterygians, with a virtual reconstruction of a new braincase of *Lawrenciella* Poplin, 1984 from the Carboniferous of Oklahoma. *Geodiversitas* **38**, 489–504.
Rayner, D. H. 1952. On the cranial structure of an early Palæoniscid, *Kentuckia*, gen. nov. *Earth and Environmental Science Transactions of the Royal Society of Edinburgh* **62**, 53–83.
Romer, A. S. 1966. *Vertebrate Paleontology*, 3rd edn. Chicago: University of Chicago Press.
Schultze, H. -P., Mickle, K. E., Poplin, C., Hilton, E. J. & Grande, L. 2021. *Handbook of Paleoichthology*, **8A**. München: Verlag Dr Friedrich Pfeil.
Smith, A. B. 1994. *Systematics and the Fossil Record*. Oxford: Blackwell Scientific Publications.
Traquair, R. H. 1877a. On the Agassizian genera Amblypterus, Palaeoniscum, Gyrolepis, and Pygopterus. *Quarterly Journal of the Geological Society* **33**, 548–78.
Traquair, R. H. 1877b. The ganoid fishes of the British Carboniferous Formations. Part I, no. 1. Palæoniscidæ. *Monographs of the Palaeontographical Society* **31**, 1–60.
Traquair, R. H. 1901. The ganoid fishes of the British Carboniferous Formations. Part I, no. 2. Palæoniscidæ. *Monographs of the Palaeontographical Society* **55**, 61–87.
Traquair, R. H. 1909. The ganoid fishes of the British Carboniferous Formations. Part I, no. 4. Palæoniscidæ. *Monographs of the Palaeontographical Society* **63**, 107–22.
Traquair, R. H. 1911. The ganoid fishes of the British Carboniferous Formations. Part I, no. 5. Palæoniscidæ. *Monographs of the Palaeontographical Society* **64**, 123–58.
Véran, M. 1988. Les éléments accessoires de l'arc hyoïdien des poissons téléostomes (Acanthodiens et Osteichthyens) fossiles et actuels. *Mémoires du Muséum National d'Histoire Naturelle* **54**, 1–98.
Wiley, E. O. 1981. *Phylogenetics. The Theory and Practice of Phylogenetic Systematics*. New York: John Wiley and Sons.
Wood, S. P. 1982. New basal Namurian (Upper Carboniferous) fishes and crustaceans found near Glasgow. *Nature* **297**, 574–77.
Woodward, A. S. 1891. *Catalogue of the Fossil Fishes in the British Museum (Natural History)*, Vol. **2**. London: British Museum (Natural History).

MS received 29 March 2024. Accepted for publication 08 November 2024